Interaction Notes

Note 133
May 1973

INDUCED CURRENTS ON A CABLE SHIELDED BY TWO UNIDIRECTIONALLY-CONDUCTING SHELLS

by

K. F. Casey
Department of Electrical Engineering
Kansas State University
Manhattan, Kansas 66506

Abstract

The axial currents and interconductor voltages induced on a coaxial-cable model are calculated when the cable is illuminated by an incident plane electromagnetic wave. The model comprises a central cylindrical conductor shielded by a concentric pair of unidirectionally-conducting shells, whose conduction angles and separation are arbitrary. In the low-frequency limit, the currents and voltages induced by the TM_z portion of the incident field are singular as $(\omega \ln \omega)^{-1}$, while those induced by the TE_z portion approach constant values as $\omega \to 0$. The shielding effectiveness parameter, defined as the ratio of the induced current on the center conductor to the total current on the structure, is determined. An equivalent transmission-line circuit incremental model is also found and its parameters expressed in terms of the physical cable parameters. Numerical results are presented to illustrate the analysis. It is found that the model characteristics approach those of an ideal coaxial cable when either shell conducts in the axial direction and/or the shell separation becomes small. Perfect shielding may also be obtained, for a cable of realistic dimensions, if the conduction angles of the shells are nearly perpendicular.

I. Introduction

The problem considered in this note is that of determining the induced currents and voltages on a particular model of a coaxial cable, when it is illuminated by an incident plane wave. The transmission-line characteristics of the model are also to be found. The objective is to model certain features of a realistic braided-conductor shield and to examine the effect of varying the model parameters on the effectiveness of the shielding and the characteristic impedance and propagation constant of the transmission-line mode.

In the present instance, the significant feature of the shield model is the existence of two preferred directions of conduction, a characteristic of grids of crossed wires. Although we are able to take into account the fact that the wires are connected in a real shield (in the sense that there is no potential difference between the unidirectionally-conducting shells), the model prohibits consideration of the finite optical coverage characteristic of an actual braid shield. As a consequence, the extent to which the structure analyzed in this note represents an actual braided-shield coaxial cable is open to some conjecture.

In Section II of this note, we obtain the frequency-domain solution for the axially symmetric part of the electromagnetic field induced by an incident plane wave. These results are specialized in Section III to the low-frequency limit, and expressions are obtained for the induced currents and voltages and the shielding effectiveness. In Section IV the characteristics of the cable as a transmission line are determined and an equivalent circuit model is obtained. Numerical results are presented in Section V; the study is summarized in Section VI.

II. Formulation of the Problem

The geometry of the problem is shown in Figs. (1) and (2). A plane electromagnetic wave is incident upon the cylindrical cable structure at an angle θ with respect to the positive z-axis (the cable axis). The electric field amplitude in the incident wave is E_o; the polarization of the incident wave is described by the angle β. If $\beta = 0°$, the incident wave is E-type (TM with respect to z); if $\beta = 90°$, it is H-type (TE with respect to z).

The cable structure comprises a central cylindrical conductor of radius a surrounded by two concentric unidirectionally-conducting cylindrical shells of radii ρ_1 and ρ_2 ($\rho_1 < \rho_2$). The conduction angles of the shells are α_1 and α_2 respectively, these angles being measured from the circumferential direction. Thus if $\alpha = 0°$, the shell conducts only in the circumferential direction; if $\alpha = 90°$, it conducts only in the axial direction. The medium between the center conductor and the inner shell is an essentially lossless ($\sigma = 0$) dielectric of permittivity ε_1. In order to model the fact that the braid wires are electrically connected in a real coaxial-cable shield, the medium between the inner and outer shells is assumed to have a finite dc conductivity σ_2. Its permittivity will be assumed to be ε_2; for simplicity, we shall write ε_2 for $\varepsilon_2(1 + \sigma_2/j\omega\varepsilon_2)$ in what follows. The permeability of each region is μ_o and the medium outside the structure is free space (ε_o,μ_o).

The time-harmonic electromagnetic field, which is assumed to vary as $\exp(j\omega t)$, is expressible in each region in terms of two scalar functions Ψ and Φ which satisfy the scalar Helmholtz equation:

$$\bar{E} = -\nabla \times \Phi \bar{a}_z + \frac{1}{j\omega\varepsilon} \nabla \times \nabla \times \Psi \bar{a}_z \qquad (1a)$$

$$\bar{H} = \nabla \times \Psi \bar{a}_z + \frac{1}{j\omega\mu} \nabla \times \nabla \times \Phi \bar{a}_z \qquad (1b)$$

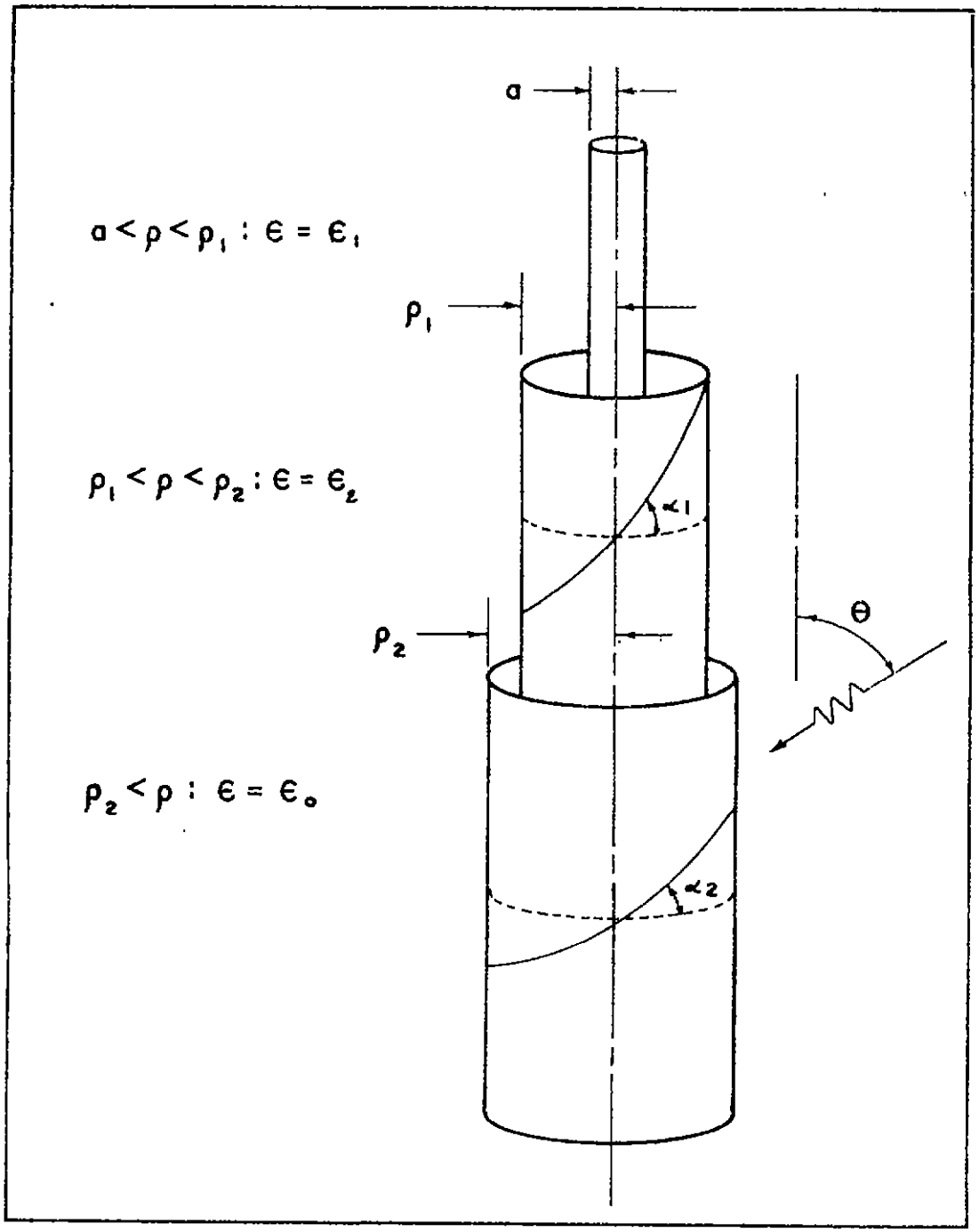

Fig. 1. Geometry of the problem: cable structure and incident wave direction.

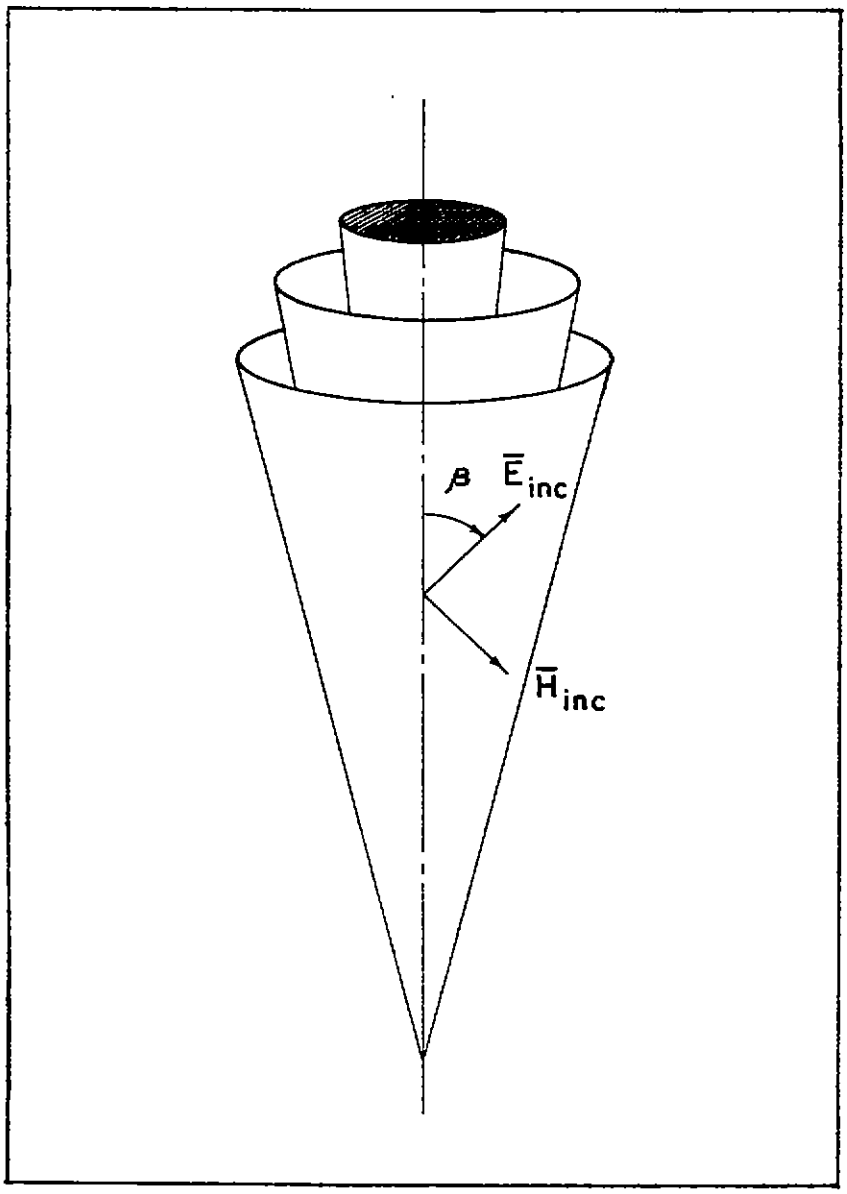

Fig. 2. Geometry of the problem: incident wave polarization.

in which $\bar{a}_z$ denotes the unit vector in the z-direction and

$$(\nabla^2 + k^2) \begin{pmatrix} \Psi \\ \Phi \end{pmatrix} = 0 \quad . \tag{2}$$

$k^2 = \omega^2 \mu\varepsilon$; Ψ and Φ generate respectively the TM and TE portions of the electromagnetic field.

It is easy to show [1] that only the axially symmetric TM portion of the electromagnetic field induces axially-directed currents on the conductors. Since it is these currents which are of principal interest, we shall henceforth consider only that part of the electromagnetic field which is independent of the azimuthal coordinate ϕ. Furthermore, since the cable structure and the plane-wave excitation are axially uniform, all field components will vary with z as $\exp(-jk_z z)$. Insofar as the induced fields are concerned, $k_z = -k_o \cos\theta$, with $k_o = \omega\sqrt{\mu_o \varepsilon_o}$. Now denote a typical axially-symmetric field quantity $A_o(\rho,z) = \hat{A}_o(\rho) \exp(-jk_z z)$; we find

$$\hat{E}_{\rho o} = \frac{-k_z}{\omega\varepsilon} \frac{d\hat{\Psi}_o}{d\rho} \qquad \hat{H}_{\rho o} = \frac{-k_z}{\omega\mu} \frac{d\hat{\Phi}_o}{d\rho}$$

$$\hat{E}_{\phi o} = \frac{d\hat{\Phi}_o}{d\rho} \qquad \hat{H}_{\phi o} = -\frac{d\hat{\Psi}_o}{d\rho} \tag{3}$$

$$\hat{E}_{zo} = \frac{k^2 - k_z^2}{j\omega\varepsilon} \hat{\Psi}_o \qquad \hat{H}_{zo} = \frac{k^2 - k_z^2}{j\omega\mu} \hat{\Phi}_o$$

in which $\hat{\Psi}_o$ and $\hat{\Phi}_o$ satisfy the zero-order Bessel equation

$$\frac{1}{\rho} \frac{d}{d\rho} \left(\rho \frac{dR}{d\rho}\right) + \lambda^2 R = 0 \; ; \tag{4}$$

$\lambda^2 = k^2 - k_z^2$ and $R = \hat{\Psi}_o$ or $\hat{\Phi}_o$. Henceforth we shall drop the "o" subscripts, understanding that only the axially-symmetric part of the field is being considered. We now construct appropriate solutions for $\hat{\Psi}$ and $\hat{\Phi}$ in each region and solve the resulting boundary-value problem.

In region 1, $a \leq \rho < \rho_1$, $\hat{\Psi}$ and $\hat{\Phi}$ are chosen as follows:

$$\hat{\Psi}^{(1)} = \frac{\hat{I}}{4} [J_o(\lambda_1\rho)Y_o(\lambda_1 a) - J_o(\lambda_1 a)Y_o(\lambda_1\rho)] \tag{5a}$$

$$\hat{\Phi}^{(1)} = \frac{\hat{I}P}{4} [J_o(\lambda_1\rho)Y_o'(\lambda_1 a) - J_o'(\lambda_1 a)Y_o(\lambda_1\rho)] \quad . \tag{5b}$$

$\lambda_1 = \sqrt{k_1^2 - k_z^2}$; $k_1^2 = \omega^2\mu_o\varepsilon_1$; primes denote differentiation with respect to the argument; $\hat{I}$ is the unknown current on the center conductor and P is a coefficient to be determined. The functional forms are chosen so that $\hat{E}_z$ and $\hat{E}_\phi$ vanish on the conducting surface $\rho = a$.

The determination of the coefficient P, as well as that of others occurring in the problem, follows from the "sheath conditions" imposed at a unidirectionally-conducting surface [2]. These conditions require that

1. The electric field component parallel to the conduction direction vanish:

$$E_z \sin\alpha + E_\phi \cos\alpha = 0 \; ; \tag{6a}$$

2. The electric field component normal to the conduction direction be continuous:

$$E_z \cos\alpha - E_\phi \sin\alpha = \text{continuous} \; ; \tag{6b}$$

3. The magnetic field component parallel to the conduction direction be continuous:

$$H_z \sin\alpha + H_\phi \cos\alpha = \text{continuous} \quad . \tag{6c}$$

If the first condition is imposed on the field components generated by $\hat{\Psi}^{(1)}$ and $\hat{\Phi}^{(1)}$ at $\rho = \rho_1$, we find the value of the coefficient P:

$$P = \frac{-\lambda_1}{j\omega\varepsilon_1} \tan\alpha_1 \frac{W_2}{W_1} \quad , \tag{7}$$

in which

$$W_1 = J_o'(\lambda_1 a)Y_o'(\lambda_1\rho_1) - J_o'(\lambda_1\rho_1)Y_o'(\lambda_1 a) \tag{8a}$$

$$W_2 = J_o(\lambda_1 a)Y_o(\lambda_1\rho_1) - J_o(\lambda_1\rho_1)Y_o(\lambda_1 a) \quad . \tag{8b}$$

This completes the solution for the fields in the inner most region to within the value of $\hat{I}$.

In region 2, $\rho_1 < \rho < \rho_2$, $\hat{\Psi}$ and $\hat{\Phi}$ are chosen to be

$$\hat{\Psi}(2) = \frac{A\hat{I}}{4}\left[J_o(\lambda_2\rho)Y_o(\lambda_2\rho_1) - J_o(\lambda_2\rho_1)Y_o(\lambda_2\rho)\right]$$

$$+ \frac{B\hat{I}}{4}\left[J_o(\lambda_2\rho)Y_o(\lambda_2\rho_2) - J_o(\lambda_2\rho_2)Y_o(\lambda_2\rho)\right] \tag{9a}$$

$$\hat{\Phi}(2) = \frac{C\hat{I}}{4}\left[J_o(\lambda_2\rho)Y_o'(\lambda_2\rho_1) - J_o'(\lambda_2\rho_1)Y_o(\lambda_2\rho)\right]$$

$$+ \frac{D\hat{I}}{4}\left[J_o(\lambda_2\rho)Y_o'(\lambda_2\rho_2) - J_o'(\lambda_2\rho_2)Y_o(\lambda_2\rho)\right] \tag{9b}$$

where $\lambda_2 = \sqrt{k_2^2 - k_z^2}$, $k_2^2 = \omega^2\mu_o\varepsilon_2$, and in which the coefficients A, B, C, D are to be determined. Applying the first sheath condition at $\rho = \rho_1$ and $\rho = \rho_2$, and the second and third sheath conditions at $\rho = \rho_1$ yields expressions for these coefficients as follows:

$$A = \frac{\pi\rho_1}{2}\left\{\cos\alpha_1\cos\alpha_2 + \frac{\lambda_2^2}{k_2^2}\frac{W_6}{W_5}\sin\alpha_1\sin\alpha_2\right\}^{-1} \quad .$$

$$\left\{\sin\alpha_1\tan\alpha_1\cos\alpha_2\frac{\lambda_1^2 W_2}{k_1^2}\left[\lambda_1\frac{W_3}{W_1} + \lambda_2\frac{W_7}{W_5}\right]\right.$$

$$\left. + \cos\alpha_1\cos\alpha_2\left[\lambda_1 W_4 + \lambda_2\frac{\varepsilon_2\lambda_1^2}{\varepsilon_1\lambda_2^2}\frac{W_2 W_8}{W_6}\right]\right\} \tag{10a}$$

$$B = -\frac{\varepsilon_2\lambda_1^2}{\varepsilon_1\lambda_2^2}\frac{W_2}{W_6} \tag{10b}$$

$$C = -\frac{\lambda_2}{j\omega\varepsilon_2} A \tan\alpha_2 \frac{W_6}{W_5} \tag{10c}$$

$$D = \frac{\lambda_2}{j\omega\varepsilon_2} \frac{\varepsilon_2\lambda_1^2}{\varepsilon_1\lambda_2^2} \frac{W_2}{W_5} \tan\alpha_1 \quad , \tag{10d}$$

in which

$$W_3 = J_o(\lambda_1\rho_1)Y_o'(\lambda_1 a) - J_o'(\lambda_1 a)Y_o(\lambda_1\rho_1) \tag{11a}$$

$$W_4 = J_o(\lambda_1 a)Y_o'(\lambda_1\rho_1) - J_o'(\lambda_1\rho_1)Y_o(\lambda_1 a) \tag{11b}$$

$$W_5 = J_o'(\lambda_2\rho_1)Y_o'(\lambda_2\rho_2) - J_o'(\lambda_2\rho_2)Y_o'(\lambda_2\rho_1) \tag{11c}$$

$$W_6 = J_o(\lambda_2\rho_1)Y_o\ \lambda_2\rho_2) - J_o(\lambda_2\rho_2)Y_o(\lambda_2\rho_1) \tag{11d}$$

$$W_7 = J_o(\lambda_2\rho_1)Y_o'(\lambda_2\rho_2) - J_o'(\lambda_2\rho_2)Y_o(\lambda_2\rho_1) \tag{11e}$$

$$W_8 = J_o(\lambda_2\rho_2)Y_o'(\lambda_2\rho_1) - J_o'(\lambda_2\rho_1)Y_o(\lambda_2\rho_2) \quad . \tag{11f}$$

This completes the solution for the fields in the region between the shells to within the value of $\hat{I}$.

In region 3, $\rho > \rho_2$, $\hat{\Psi}$ and $\hat{\Phi}$ are given by

$$\hat{\Psi}(3) = \frac{j\omega\varepsilon_o E_o}{\lambda_o^2} \sin\theta \cos\beta\ J_o(\lambda_o\rho) + QH_o^{(2)}(\lambda_o\rho) \tag{12a}$$

$$\hat{\Phi}(3) = \frac{-j\omega\mu_o E_o}{\lambda_o^2\eta_o} \sin\theta \sin\beta\ J_o(\lambda_o\rho) + SH_o^{(2)}(\lambda_o\rho) \quad , \tag{12b}$$

in which the scattered-wave amplitudes Q and S are unknown; $\lambda_o = \sqrt{k_o^2 - k_z^2}$ and $\eta_o = \sqrt{\mu_o/\varepsilon_o}$ denotes the characteristic impedance of free space. Applying each of the sheath conditions at $\rho = \rho_2$ permits a solution for $\hat{I}$, Q, and S to be obtained in terms of the incident field amplitude E_o. We obtain for $\hat{I}$:

$$\hat{I} = \frac{8k_o E_o \cos\alpha_2 \sin^2\theta}{\pi\rho_o \Delta} \left[j \cos\alpha_2 \cos\beta H_o^{(2)'}(\lambda_o\rho_2) \right.$$

$$\left. - \sin\alpha_2 \sin\theta \sin\beta H_o^{(2)}(\lambda_o\rho_2) \right] \qquad (13)$$

in which

$$\Delta = \frac{AW_6\lambda_2^2\lambda_o^2}{j\omega\varepsilon_2} \left[\cos^2\alpha_2 H_o^{(2)'}(\lambda_o\rho_2)^2 - \sin^2\alpha_2 \sin^2\theta H_o^{(2)}(\lambda_o\rho_2)^2 \right]$$

$$- F \frac{\lambda_o^3}{j\omega\varepsilon_o} \cos\alpha_2 H_o^{(2)}(\lambda_o\rho_2) H_o^{(2)'}(\lambda_o\rho_2) \quad . \qquad (14)$$

A is given in eq. (10a) and

$$F = \lambda_2 \cos\alpha_2 \left(AW_7 - \frac{2}{\pi\lambda_2\rho_2} \frac{\varepsilon_2\lambda_1^2}{\varepsilon_1\lambda_2^2} \frac{W_2}{W_6} \right)$$

$$+ \frac{\lambda_2^2}{j\omega\mu_o} \sin\alpha_2 \left(CW_8 + \frac{\lambda_2}{j\omega\varepsilon_2} \frac{\varepsilon_2\lambda_1^2}{\varepsilon_1\lambda_2^2} \frac{W_2}{W_5} \frac{2}{\pi\lambda_2\rho_2} \tan\alpha_1 \right) . \qquad (15)$$

The TM scattered-field amplitude factor Q is given by

$$Q = \frac{-1}{H_o^{(2)}(\lambda_o\rho_2)} \left\{ \frac{j\omega\varepsilon_o E_o}{\lambda_o^2} \cos\beta \sin\theta J_o(\lambda_o\rho_2) + \frac{\varepsilon_o\lambda_2^2}{4\varepsilon_2\lambda_o^2} AW_6\hat{I} \right\} \quad . \qquad (16)$$

The TE scattered-field amplitude factor S is not of interest and is not considered further. This completes the formal solution for the axially symmetric field quantities.

In the following section we obtain expressions for the induced currents and voltages valid in the low-frequency limit.

III. Induced Currents and Voltages in the Low-Frequency Limit

It is convenient to treat the cases $\beta = 0°$ (TM incident wave) and $\beta = 90°$ (TE incident wave) separately. We shall denote the currents with appropriate superscripts and consider the TM case first.

In the low-frequency limit, the values of the expressions W_1 through W_8 become

$$W_1 \to W_{10} = \frac{1}{\pi}\left(\frac{\rho_1}{a} - \frac{a}{\rho_1}\right) \tag{17a}$$

$$W_2 \to W_{20} = \frac{2}{\pi} \ln \frac{\rho_1}{a} \tag{17b}$$

$$W_3 \to W_{30} = \frac{2}{\pi\lambda_1 a} \tag{17c}$$

$$W_4 \to W_{40} = \frac{2}{\pi\lambda_1\rho_1} \tag{17d}$$

$$W_5 \to W_{50} = \frac{1}{\pi}\left(\frac{\rho_2}{\rho_1} - \frac{\rho_1}{\rho_2}\right) \tag{17e}$$

$$W_6 \to W_{60} = \frac{2}{\pi} \ln \frac{\rho_2}{\rho_1} \tag{17f}$$

$$W_7 \to W_{70} = \frac{2}{\pi\lambda_2\rho_2} \tag{17g}$$

$$W_8 \to W_{80} = \frac{2}{\pi\lambda_2\rho_1} \quad . \tag{17h}$$

In this limit, the coefficients A, B, C, D, P, and F are constants with respect to frequency, given by

$$A \to A_o = \left(\cos\alpha_1 \cos\alpha_2 + \frac{W_{60}}{W_{50}} \sin\alpha_1 \sin\alpha_2\right)^{-1} \cdot$$

$$\left\{\cos\alpha_1 \cos\alpha_2 \left[1 + \frac{\lambda_1^2}{k_1^2} \frac{W_{20}}{W_{60}}\right]\right.$$

$$\left. + \frac{\lambda_1^2}{k_1^2} \sin\alpha_1 \tan\alpha_1 \cos\alpha_2 \left[\frac{\rho_1 W_{20}}{aW_{10}} + \frac{\rho_1 W_{20}}{\rho_2 W_{50}}\right]\right\} \quad \dagger \qquad (18a)$$

$$B \to B_o = \frac{-\lambda_1^2 W_{20}}{k_1^2 W_{60}} \qquad (18b)$$

$$C \to 0 \qquad (18c)$$

$$D \to 0 \qquad (18d)$$

$$P \to P_o = \frac{-\lambda_1}{j\omega\varepsilon_1} \tan\alpha_1 \frac{W_{20}}{W_{10}} \qquad (18e)$$

$$F \to F_o = \left(\cos\alpha_1\cos\alpha_2 + \frac{W_{60}}{W_{50}} \sin\alpha_1 \sin\alpha_2\right)^{-1} \cdot \left[\frac{2}{\pi\rho_2\cos\alpha_1}\right] \cdot$$

$$\left\{\left[\frac{\rho_2}{a} \frac{W_{60}}{W_{50}} \sin^2\alpha_2 + \frac{\rho_1}{a} \cos^2\alpha_2\right]\left[\frac{W_{20}}{W_{10}} \frac{\lambda_1^2}{k_1^2} \sin^2\alpha_1 + \frac{a}{\rho_1} \cos^2\alpha_1\right]\right.$$

$$\left. + \frac{\lambda_1^2}{k_1^2} \frac{W_{20}}{W_{50}} \frac{\rho_1}{\rho_2} \left[\sin\alpha_1 \cos\alpha_2 - \frac{\rho_2}{\rho_1} \sin\alpha_2 \cos\alpha_1\right]^2\right\} . \qquad (18f)$$

In the low-frequency limit, the dominant term in Δ, given in eq. (14), is

$$\Delta \to \Delta_o = \frac{-\lambda_o^3 F_o}{j\omega\varepsilon_o} \cos\alpha_2 \, H_o^{(2)}(\lambda_o\rho_2) H_o^{(2)'}(\lambda_o\rho_2) \quad . \qquad (19)$$

We may now consider separately the two cases mentioned above.

---

†In this and the expressions to follow, we have used the fact that $\varepsilon_2(1 + \sigma_2/j\omega\varepsilon_2) \to -j\infty$ as $\omega \to 0$.

$\beta = 0°$: TM excitation

If $\beta = 0°$, one uses the various limiting forms given above to show that

$$\hat{I}^{TM} \to \hat{I}_o^{TM} = \frac{4E_o \cos\alpha_2}{\left(\frac{\pi\rho_2}{2}\right)\eta_o\lambda_o H_o^{(2)}(\lambda_o\rho_2) F_o} ; \tag{20}$$

it is apparent that $\hat{I}_o^{TM}$ is singular as $(\omega \ln \omega)^{-1}$. It will be noted that this behavior is identical to that of the current induced on a bare conductor. Thus the TM-induced component of the time-domain current on the center conductor may be found using the results obtained by Barnes [1].

The total cable current in the limit, $\hat{I}_{to}^{TM}$, is given by

$$\begin{aligned}\hat{I}_{to}^{TM} &= \lim_{\omega\to 0} 2\pi\rho_2 H_\phi^{(3)}(\rho_2)\big|_{\beta=0} \\ &= \lim_{\omega\to 0} -2\pi\rho_2 \left.\frac{d\hat{\psi}^{(3)}}{d\rho}\right|_{\rho=\rho_2,\ \beta=0} \\ &= \frac{4E_o}{\eta_o\lambda_o H_o^{(2)}(\lambda_o\rho_2)} .\end{aligned} \tag{21}$$

Now defining a "shielding effectiveness parameter" $r^{TM} = \hat{I}_o^{TM}/\hat{I}_{to}^{TM}$, we find

$$r^{TM} = \frac{\cos\alpha_1 \cos\alpha_2 \left(\cos\alpha_1 \cos\alpha_2 + \frac{W_{60}}{W_{50}} \sin\alpha_1 \sin\alpha_2\right)}{\left\{\left(\frac{\rho_2}{\rho_1}\frac{W_{60}}{W_{50}} \sin^2\alpha_2 + \cos^2\alpha_2\right)\left(\frac{W_{20}}{W_{10}}\frac{\lambda_1^2}{k_1^2}\frac{\rho_1}{a} \sin^2\alpha_1 + \cos^2\alpha_1\right)\right.}$$

$$\left. + \frac{\lambda_1^2}{k_1^2}\frac{W_{20}}{W_{50}}\frac{\rho_1}{\rho_2}\left(\sin\alpha_1 \cos\alpha_2 - \frac{\rho_2}{\rho_1}\sin\alpha_2 \cos\alpha_1\right)^2\right\} . \tag{22}$$

As a partial check, consider r^{TM} in the special case $\alpha_2 = \alpha_1$, $\theta = 90°$, and $\rho_2 = \rho_1$. This corresponds to a single unidirectionally conducting shell and normal incidence of the illuminating wave. We find

$$r^{TM} \to \left[1 + 2 \ln \frac{\rho_1}{a} \left(\frac{\rho_1^2}{\rho_1^2 - a^2}\right) \tan^2 \alpha_1\right]^{-1} \qquad (23)$$

which is identical, except for notational differences, to the result obtained by Latham for this case [3].

$\beta = 90°$: TE excitation

If $\beta = 90°$, one uses the various limiting forms given to show that

$$\hat{I}^{TE} \to \hat{I}_o^{TE} = \frac{-4\, E_o \sin\theta \sin\alpha_2}{\eta_o F_o}$$

$$= -2\pi\rho_2 \left(\frac{E_o}{\eta_o}\right) \sin\theta \tan\alpha_2\, r^{TM} \qquad (24)$$

and that

$$\hat{I}_t^{TE} \to \hat{I}_{to}^{TE} = \frac{-4j\, A_o\, W_{60}\, \hat{I}_o^{TE}}{H_o^{(2)}(\lambda_o\rho_2) \sin^2\theta} \to 0 \quad . \qquad (25)$$

Thus a plane wave of TE polarization induces no net cable current; the inner-conductor current is a constant with respect to frequency in the low-frequency limit. Hence unless $\beta = 90°$, the induced current from the TM part of the incident wave is dominant in this limit. The induced current on the center conductor is thus given essentially by the expression (20) multiplied by $\cos\beta$; the total cable current is given by the expression (21) multiplied by $\cos\beta$, when $\beta \neq 90°$.

It is of interest to point out those conditions under which perfect shielding is obtained. These are, from eqs. (22) and (24), the following:

(1) $\cos\alpha_1 = 0$: the inner shell conducts in the axial direction; $I_o^{TM} = I_o^{TE} = 0$.

(2) $\cos\alpha_2 = 0$: the outer shell conducts in the axial direction; $I_o^{TM} = 0$, but $I_o^{TE} \neq 0$.

(3) $\sin\alpha_2 = 0$: the outer shell conducts in the circumferential direction; $I_o^{TM} \neq 0$, but $I_o^{TE} = 0$.

(4) $\cos\alpha_1\cos\alpha_2 + \frac{W_{60}}{W_{50}} \sin\alpha_1\sin\alpha_2 = 0$; $I_o^{TM} = I_o^{TE} = 0$.

(5) $\rho_2 = \rho_1$, $\alpha_1 \neq \alpha_2$; $I_o^{TE} = I_o^{TM} = 0$.

Condition (5) reflects the fact that the two shells with zero separation provide infinite conductivity in an arbitrary tangential direction and thus form a perfect shield. In a realistic shield, condition (4) above is essentially equivalent to $\cos(\alpha_1 - \alpha_2) = 0$. This occurs because the factor W_{60}/W_{50}, which depends only on the ratio ρ_2/ρ_1, is unity when $\rho_2/\rho_1 = 1$ and drops only to 0.9241 when $\rho_2/\rho_1 = 2$ (which is a thick shield indeed!). Thus perfect shielding is obtained when the conduction directions are mutually perpendicular, for a cable of realistic dimensions.

Induced voltages and shield currents

We may now consider the induced interconductor voltages. The voltage between the center conductor and the inner shell $\hat{V}_{co}$ is defined as follows, in the low-frequency limit:

$$\hat{V}_{co} = \int_{\rho=a}^{\rho_1} \hat{E}_\rho \, d\rho = \frac{k_z}{\omega\varepsilon_1} [\hat{\psi}^{(1)}(a) - \hat{\psi}^{(1)}(\rho_1)]$$

$$= \frac{k_z \hat{I}_o}{2\pi\omega\varepsilon_1} \ln \rho_1/a$$

$$= \frac{-k_o \cos\theta \, \hat{I}_o}{2\pi\omega\varepsilon_1} \ln \rho_1/a \quad . \tag{26}$$

The voltage between the inner and outer shells $\hat{V}_{so}$ is given by

$$\hat{V}_{so} = \int_{\rho_1}^{\rho_2} \hat{E}_\rho \, d\rho = \frac{k_z}{\omega\varepsilon_1} \left[\hat{\psi}^{(2)}(\rho_1) - \hat{\psi}^{(2)}(\rho_2)\right]$$

$$= 0 \, . \tag{27}$$

The fact that $\hat{V}_{so}$ vanishes in the low-frequency limit is a consequence of the fact that we have assumed a non-zero dc conductivity in the region between the shells. Thus this assumption is necessary in order to obtain a realistic model of an actual braided shield. The thickness of the shield region $\rho_1 \leq \rho \leq \rho_2$ is assumed to be much less than a skin depth, so there is no power absorbed in the shield over the frequency range of interest.

The currents on the two shells $\hat{I}_{s1}$ and $\hat{I}_{s2}$ are given by

$$\hat{I}_{s1} = \hat{I}_o(A_o + B_o - 1) \tag{28a}$$

$$\hat{I}_{s2} = \hat{I}_{to} - \hat{I}_o(A_o + B_o) \; ; \tag{28b}$$

but since the voltage between these two conductors is zero, we need not consider the currents separately. The total shield current $\hat{I}_{so}$ is simply

$$\hat{I}_{so} = \hat{I}_{to} - \hat{I}_o \, . \tag{29}$$

This completes the derivation of expressions for the induced voltages and currents in the low-frequency limit. In the following subsection, we present some special-case results for the shielding effectiveness factor r^{TM}.

Shielding effectiveness factor r^{TM}: special cases

The two special cases we shall consider are a) the counterwound cable, $\alpha_2 = -\alpha_1 = -\alpha$; and b) the cable with thin shield, $\rho_2/\rho_1 - 1 \ll 1$. Both cases are of substantial practical interest. The results for r^{TM} are given below:

a) counterwound cable:

$$r^{TM} = \frac{\cos^2\alpha\left(\cos^2\alpha - \frac{W_{60}}{W_{50}}\sin^2\alpha\right)}{\left\{\left(\frac{\rho_2}{\rho_1}\frac{W_{60}}{W_{50}}\sin^2\alpha + \cos^2\alpha\right)\left(\frac{\rho_1}{a}\frac{\lambda_1^2}{k_1^2}\frac{W_{20}}{W_{10}}\sin^2\alpha + \cos^2\alpha\right)\right.}$$

$$\left. + \frac{\lambda_1^2}{k_1^2}\frac{W_{20}}{W_{50}}\sin^2\alpha\cos^2\alpha\left(\sqrt{\frac{\rho_1}{\rho_2}} + \sqrt{\frac{\rho_2}{\rho_1}}\right)^2\right\} \tag{30}$$

b) thin shield: $\xi \equiv \rho_2/\rho_1 - 1 << 1$.

$$r^{TM} = \frac{\xi\cos\alpha_1\cos\alpha_2\cos(\alpha_1 - \alpha_2)}{\left\{\xi\left(\frac{\rho_1}{a}\frac{W_{20}}{W_{10}}\frac{\lambda_1^2}{k_1^2}\sin^2\alpha_1 + \cos^2\alpha_1\right) + \right.}$$

$$\left. \frac{\pi\lambda_1^2}{2k_1^2}W_{20}\left(\sqrt{\frac{\rho_1}{\rho_2}}\sin\alpha_1\cos\alpha_2 - \sqrt{\frac{\rho_2}{\rho_1}}\sin\alpha_2\cos\alpha_1\right)^2\right\} \tag{31}$$

a) and b): counterwound cable with thin shield:

$$r^{TM} = \frac{\xi\cos^2\alpha\left(\cot^2\alpha - 1\right)}{\xi\left(\cot^2\alpha + \frac{\rho_1}{a}\frac{W_{20}}{W_{10}}\frac{\lambda_1^2}{k_1^2}\right) + 2\pi W_{20}\cos^2\alpha\frac{\lambda_1^2}{k_1^2}} \tag{32}$$

The result (32) is of most interest from a practical standpoint, since it corresponds to most realistic cable geometries.

In the following section, we consider the characteristics of the coaxial-cable model as a transmission line.

IV. Transmission-Line Characteristics of the Model

In this section we shall consider the behavior of the coaxial cable model operating in its transmission-line mode. The propagation constant k_{zt} for this mode is obtained by setting the denominator of the expression on the right-hand side of eq. (22) equal to zero. We find that

$$k_{zt}^2/k_1^2 = 1 + \frac{\cos^2\alpha_1\left(\frac{\rho_2}{\rho_1}\frac{W_{60}}{W_{50}}\sin^2\alpha_2 + \cos^2\alpha_2\right)}{\left\{\frac{W_{20}}{W_{50}}\left(\sqrt{\frac{\rho_1}{\rho_2}}\sin\alpha_1\cos\alpha_2 - \sqrt{\frac{\rho_2}{\rho_1}}\sin\alpha_2\cos\alpha_1\right)^2 + \frac{\rho_1}{a}\frac{W_{20}}{W_{10}}\sin^2\alpha_1\left(\frac{\rho_2}{\rho_1}\frac{W_{60}}{W_{50}}\sin^2\alpha_2 + \cos^2\alpha_2\right)\right\}} . \quad (33)$$

Incorporating the assumptions that the cable shield is counterwound and thin, we obtain

$$k_{zt}^2/k_1^2 = 1 + \frac{\xi\cot^2\alpha}{\ln\rho_1/a\ \left[4\cos^2\alpha + 2\xi\left(1 - \frac{a^2}{\rho_1^2}\right)^{-1}\right]} . \quad (34)$$

The result (34) indicates that $k_{zt} \to \infty$ as $\alpha \to 0$; and $k_{zt} \to k_1$ as $\alpha \to 90°$ and/or $\xi \to 0$. It is interesting to note that under the assumptions used to derive the expression (34), $r^{TM} = 0$ if $\cot^2\alpha = 1$, but $k_{zt} \neq k_1$ in this case.

The transmission-line parameters for the structure are readily found. Considering the total cable current I_{to} as a source term in the voltage-change equation, we have[†]

$$\frac{dV_{co}}{dz} = -j\omega(L_i I_o - L_e I_{to}) , \quad (35)$$

where L_i is the "internal" and L_e the "external" inductance per meter of the cable. With the help of eq. (26), we obtain

[†]The case where $I_{to} = 0$ by virtue of the fact that $\beta = 90°$ (TE excitation) is considered in the Appendix.

$$L_i = \frac{\mu_o}{2\pi} \ln \rho_1/a \; (k_{zt}^2/k_1^2) \tag{36}$$

$$L_e = r_1^{TM} L_i \tag{37}$$

where r_1^{TM} denotes r^{TM} as given in (22), (30), (31), or (32) with $\theta = 90°$ ($\lambda_1^2 = k_1^2$). Using eqs. (22), (33), (36), and (37) we obtain for L_e in general

$$L_e = \left(\frac{\mu_o}{2\pi}\right) \frac{\cos\alpha_1 \cos\alpha_2 \left(\cos\alpha_1\cos\alpha_2 + \frac{W_{60}}{W_{50}} \sin\alpha_1 \sin\alpha_2\right)}{\left\{\frac{2}{\pi W_{50}} \left(\sqrt{\frac{\rho_1}{\rho_2}} \sin\alpha_1\cos\alpha_2 - \sqrt{\frac{\rho_2}{\rho_1}} \sin\alpha_2\cos\alpha_1\right)^2 \right.}$$

$$\left. + \frac{2\rho_1}{\pi a W_{10}} \sin^2\alpha_1 \left\{\frac{\rho_2}{\rho_1} \frac{W_{60}}{W_{50}} \sin^2\alpha_2 + \cos^2\alpha_2\right\}\right\} \quad . \tag{38}$$

For the case of the counterwound cable with small shell separation,

$$L_e = \left(\frac{\mu_o}{2\pi}\right) \frac{\xi \cos^2\alpha(\cot^2\alpha - 1)}{4\cos^2\alpha + 2\xi(1 - a^2/\rho_1^2)^{-1}} \quad . \tag{39}$$

The current-change equation is simply

$$\frac{dI_o}{dz} = \frac{-2\pi j\omega\epsilon_1}{\ln \rho_1/a} V_{co}$$

$$\equiv -j\omega C V_{co} \quad , \tag{40}$$

in which C denotes the capacity per meter of the line; hence from (35), (36), and (40), the line characteristic impedance Z_o is given by

$$Z_o = \frac{\eta_1}{2\pi} \ln \frac{\rho_1}{a} \left(\frac{k_{zt}}{k_1}\right) \quad , \tag{41}$$

with $\eta_1 = \sqrt{\mu_o/\epsilon_1}$.

From the transmission-line equations (35) and (40) we construct the equivalent circuit for a length ΔZ of the line shown in Fig. (3). The

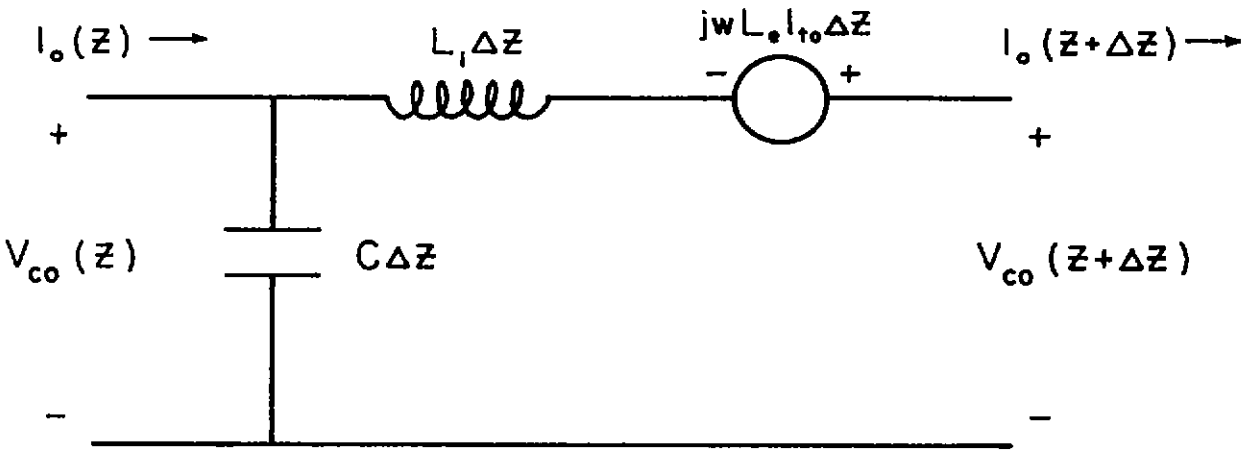

Fig. 3. Equivalent circuit for an incremental length ΔZ.

imperfect shielding of the cable is manifest in the presence of the voltage source $j\omega L_e I_{to} \Delta Z$ in series with the internal inductance $L_i \Delta Z$. We may also use the transmission-line formulas to construct an expression for r^{TM} which uses the line parameters directly. Defining $L_o = \frac{\mu_o}{2\pi} \ln \rho_1/a$, the internal inductance per unit length of an ideal coaxial cable, we have

$$r^{TM} = \frac{L_e/L_o}{L_i/L_o - \cos^2\theta/\varepsilon_{r1}} \quad , \tag{42}$$

where $\varepsilon_{r1} = \varepsilon_1/\varepsilon_0$.

In the following section, we present and discuss the results of some illustrative numerical computations.

V. Numerical Results

We have carried out numerical computation of $k_{zt}^2/k_1^2 = L_1/L_o$, and L_e/L_o. These quantities are the ratios of the internal inductance per unit length and the external inductance per unit length to the internal inductance per unit length of an ideal coaxial cable. Using eq. (42), the shielding effectiveness parameter may be readily calculated for any combination of θ and ε_{r1} desired (note that $0 \leq \cos^2\theta/\varepsilon_{r1} \leq 1$).

Each of the calculated quantities depends on the four geometrical parameters α_1, α_2, ρ_1/a, and ρ_2/ρ_1. We shall restrict attention to the counterwound case as being of the greatest practical interest, thereby reducing the number of parameters to three. The results for this case are presented in Figs. (4)-(19).

In Figs. (4)-(7) we show the variation of L_1/L_o vs. α for $\rho_2/\rho_1 = 1.1$, 1.2, 1.3, 1.4, and 1.5 and $\rho_1/a = 2.0$, 3.0, 4.0, and 5.0. L_e/L_o vs. α for the same parameter values is shown in Figs. (8)-(11). One will note that, as the equations predict, the line characteristics more nearly approach those of the ideal coaxial cable as ρ_1/a increases and/or ρ_2/ρ_1 decreases. In order to show more detail in the curves of L_e/L_o vs. α, we have shown segments of these curves ($\alpha \geq 30°$) with an expanded ordinate scale in Figs. (12)-(15). The vanishing of L_e/L_o for α near 45° is evident.

In order to show the variation in the shielding effectiveness parameter r^{TM} with the angle of incidence θ and the relative permittivity ε_{r1}, curves of r^{TM} vs. $(\cos\theta)/\sqrt{\varepsilon_{r1}}$ for $\rho_1/a = 3.0$ and 5.0, $\rho_2/\rho_1 = 1.1$ and 1.3, and various values of α are given in Figs. (16)-(19). One will notice from the curves in the figures, as well as from eq. (42), that for a given angle of incidence $\theta \neq 90°$, the shielding is improved as ε_{r1} is increased. The worst possible shielding occurs when $\theta = 0$ and $\varepsilon_{r1} = 1$; r^{TM} is in this worst case given by

$$r^{TM} = \frac{1 + \frac{W_{60}}{W_{50}} \tan\alpha_1 \tan\alpha_2}{1 + \frac{W_{60}}{W_{50}} \tan^2\alpha_2} \; ; \tag{43}$$

or if the cable is counterwound with thin shield,

$$r^{TM} = \cos 2\alpha \quad . \tag{44}$$

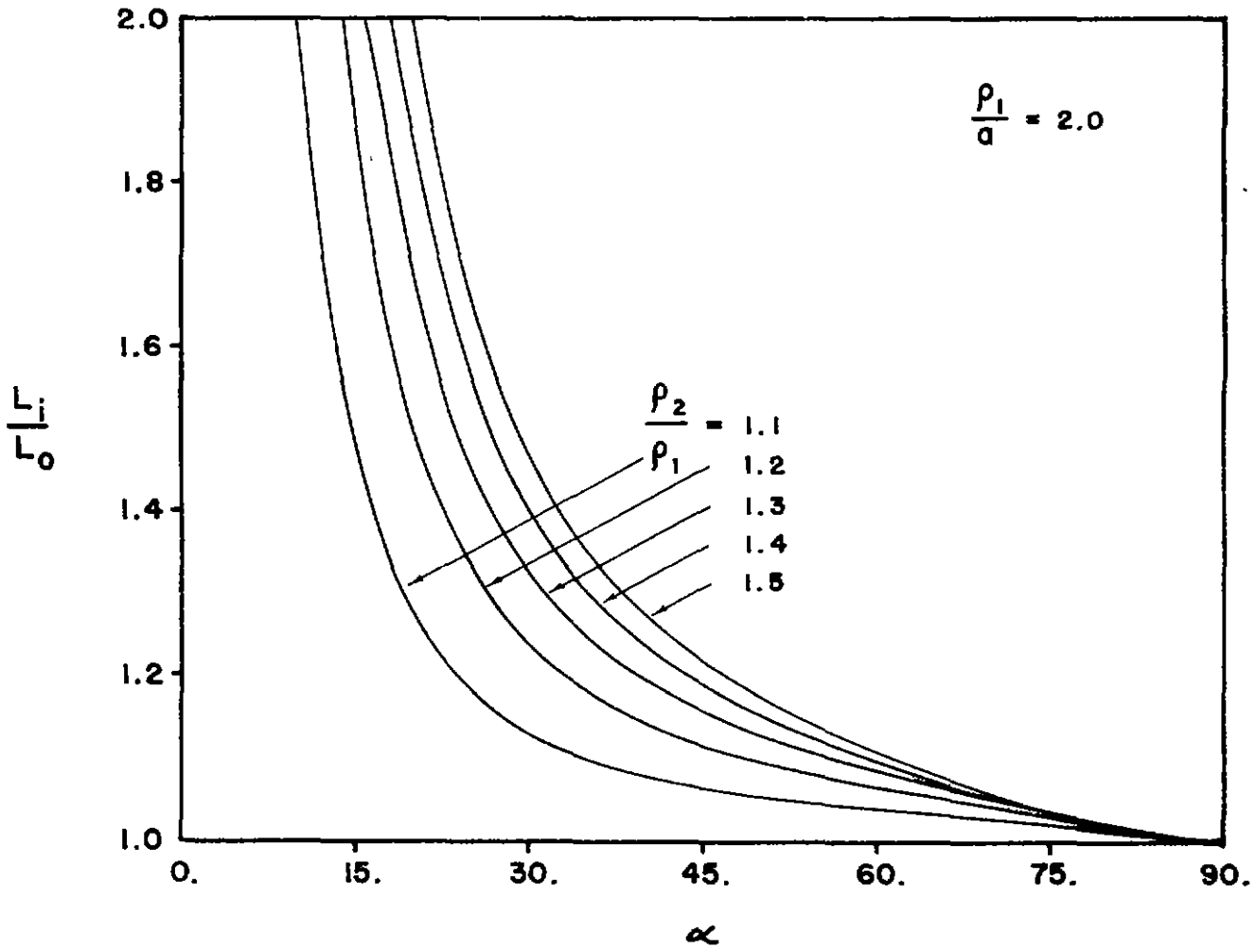

Fig. 4. Normalized internal inductance per meter vs. α: $\rho_1/a = 2.0$.

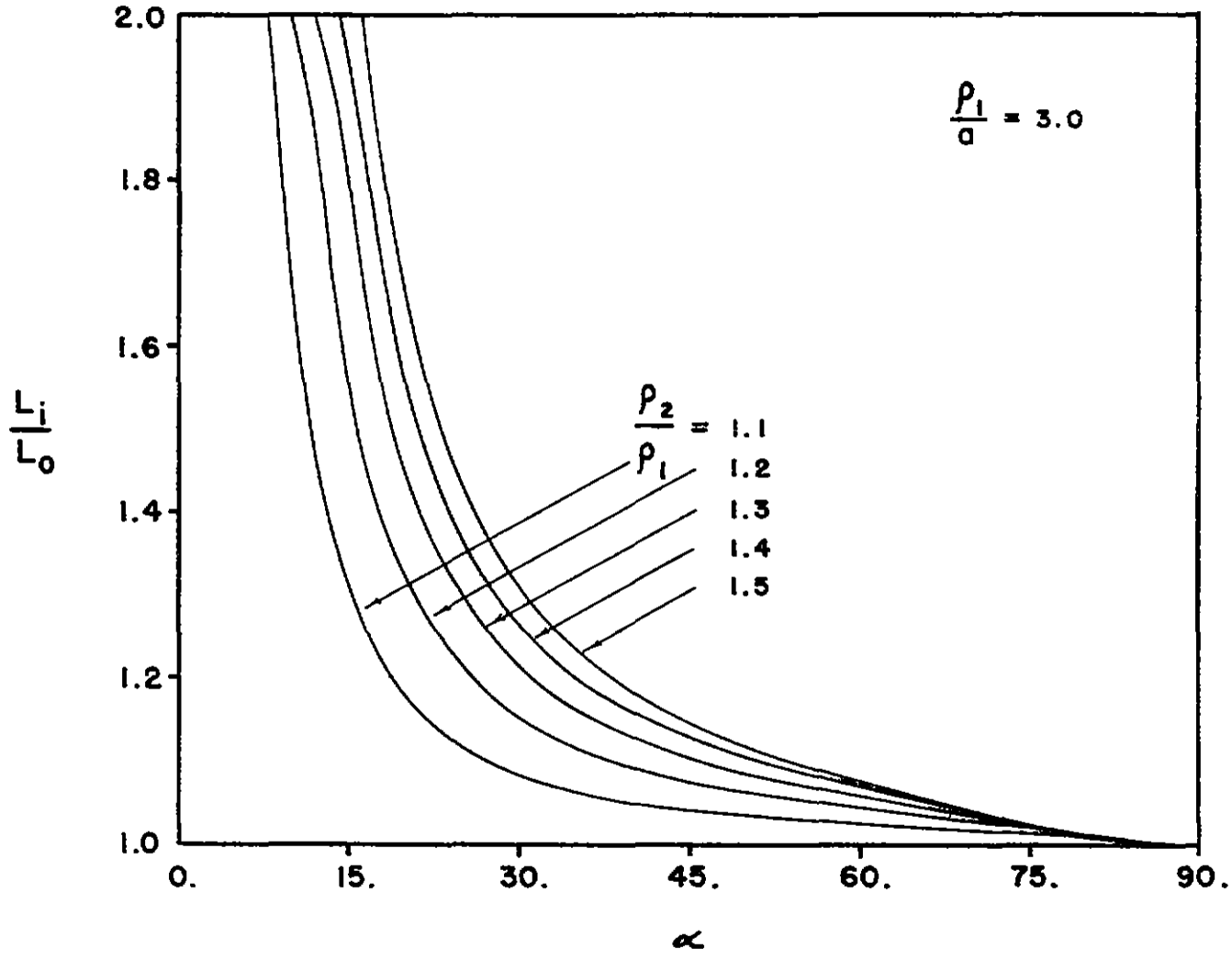

Fig. 5. Normalized internal inductance per meter vs. α: $\rho_1/a = 3.0$.

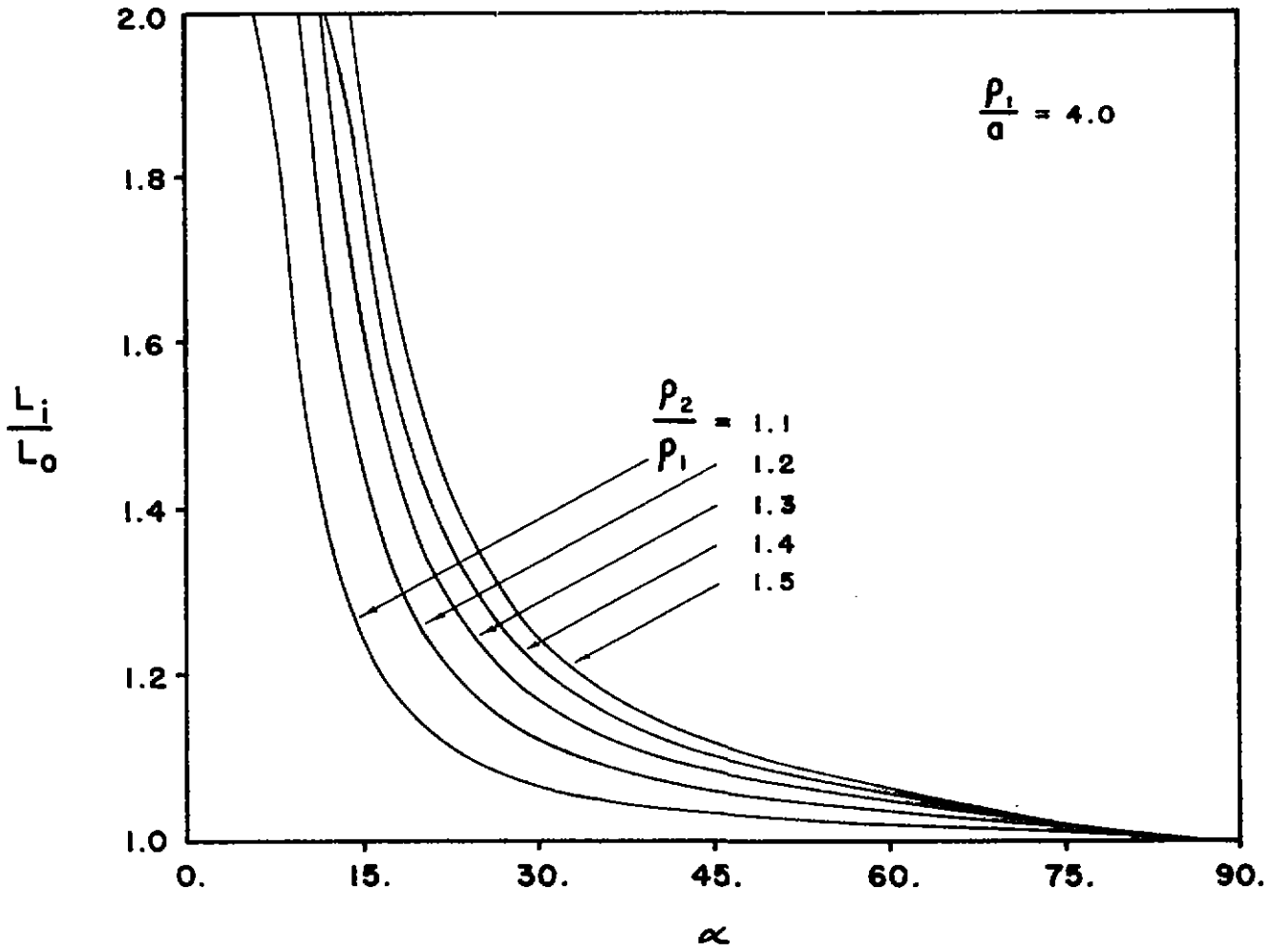

Fig. 6. Normalized internal inductance per meter vs. α: $\rho_1/a = 4.0$.

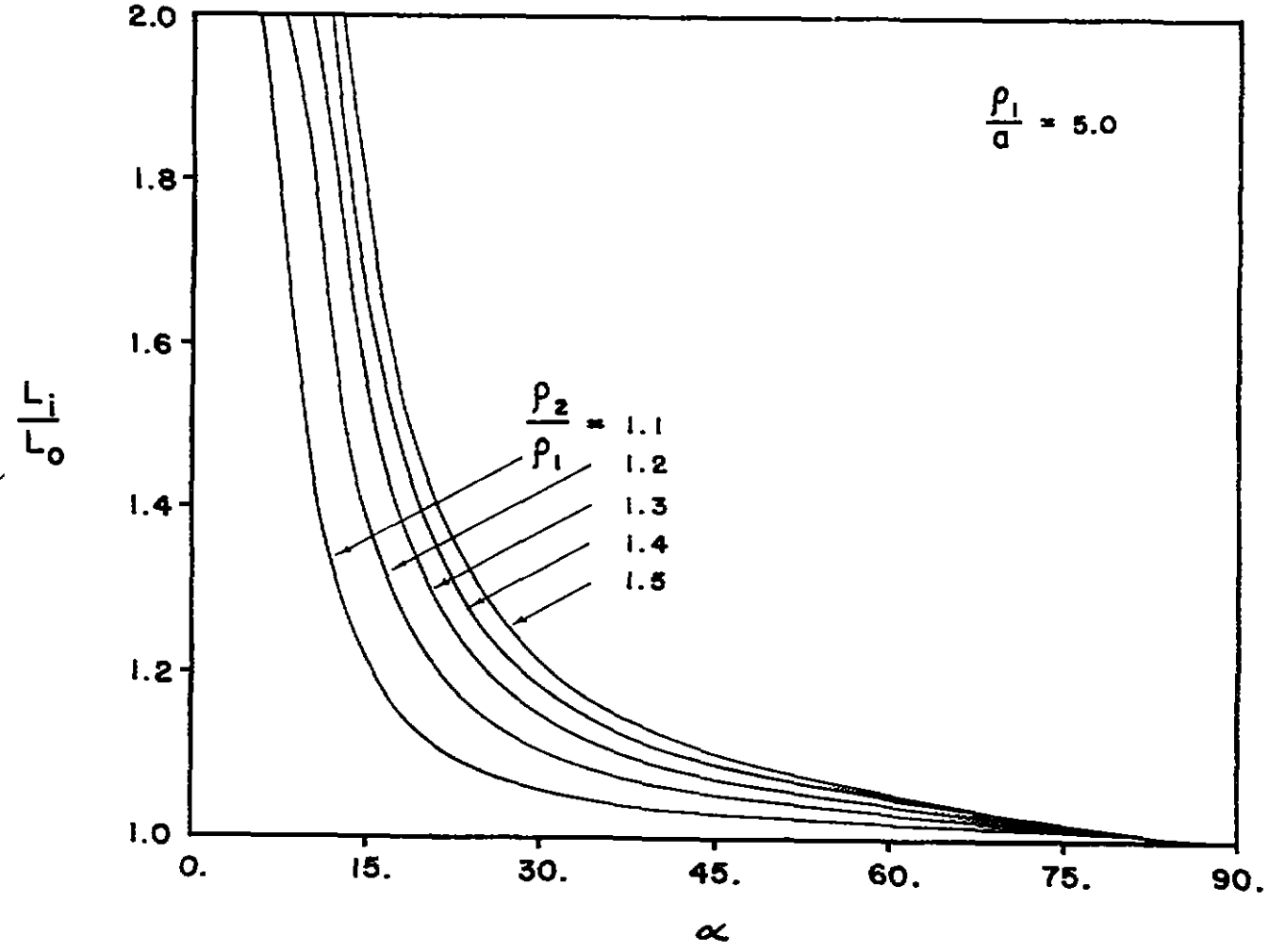

Fig. 7. Normalized internal inductance per meter vs. α: $\rho_1/a = 5.0$.

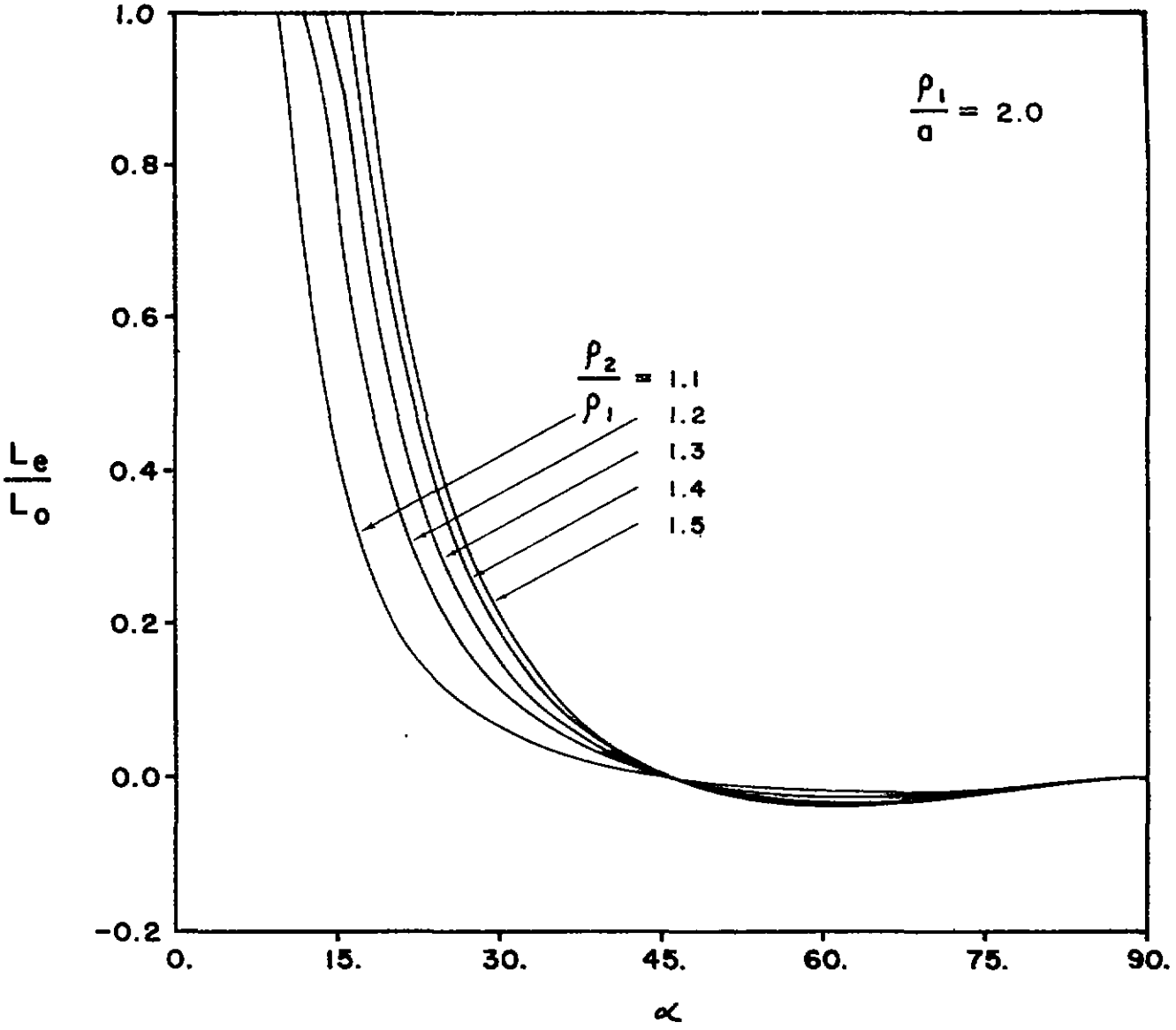

Fig. 8. Normalized external inductance per meter vs. α: $\rho_1/a = 2.0$.

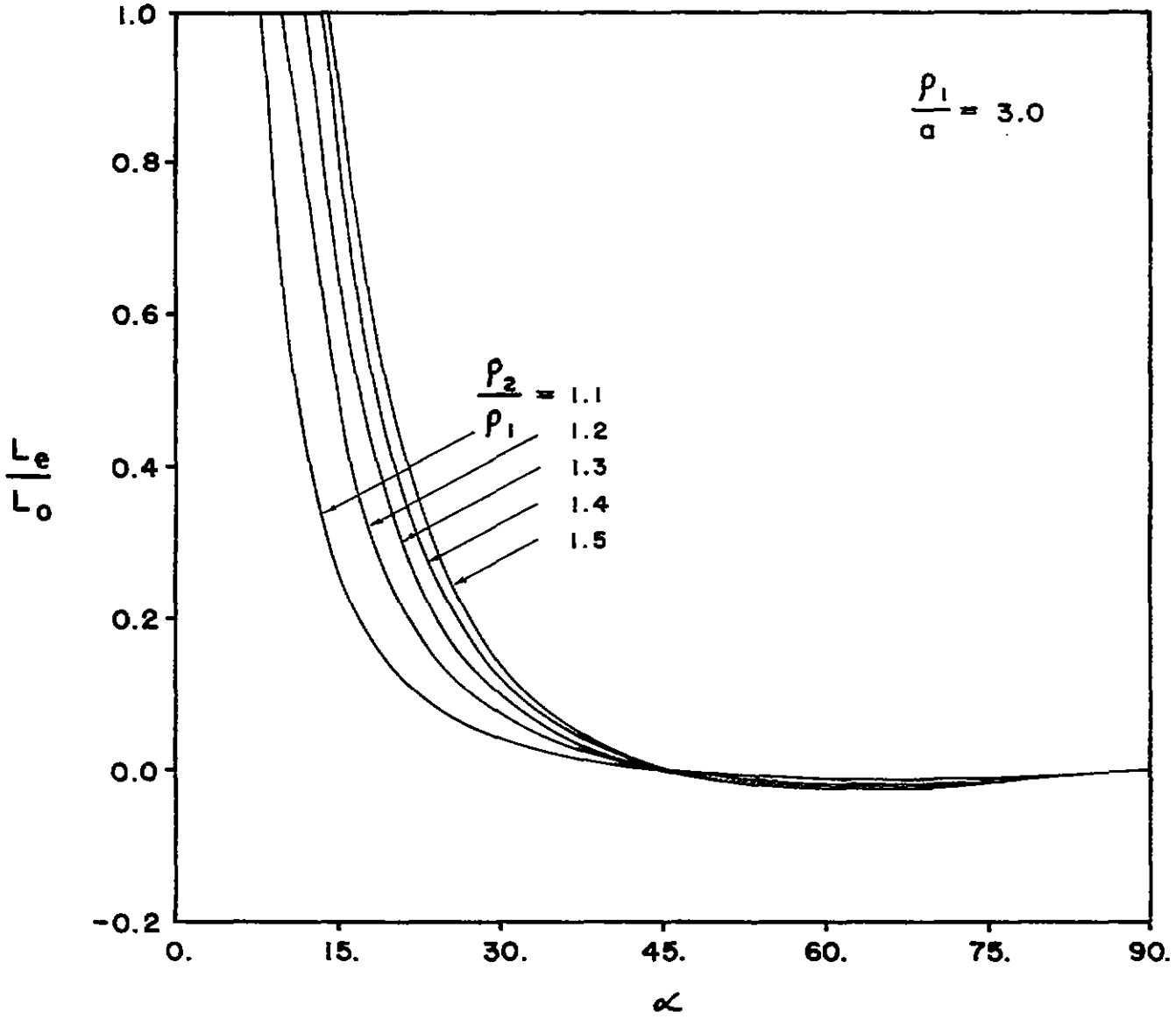

Fig. 9. Normalized external inductance per meter vs. α: $\rho_1/a = 3.0$.

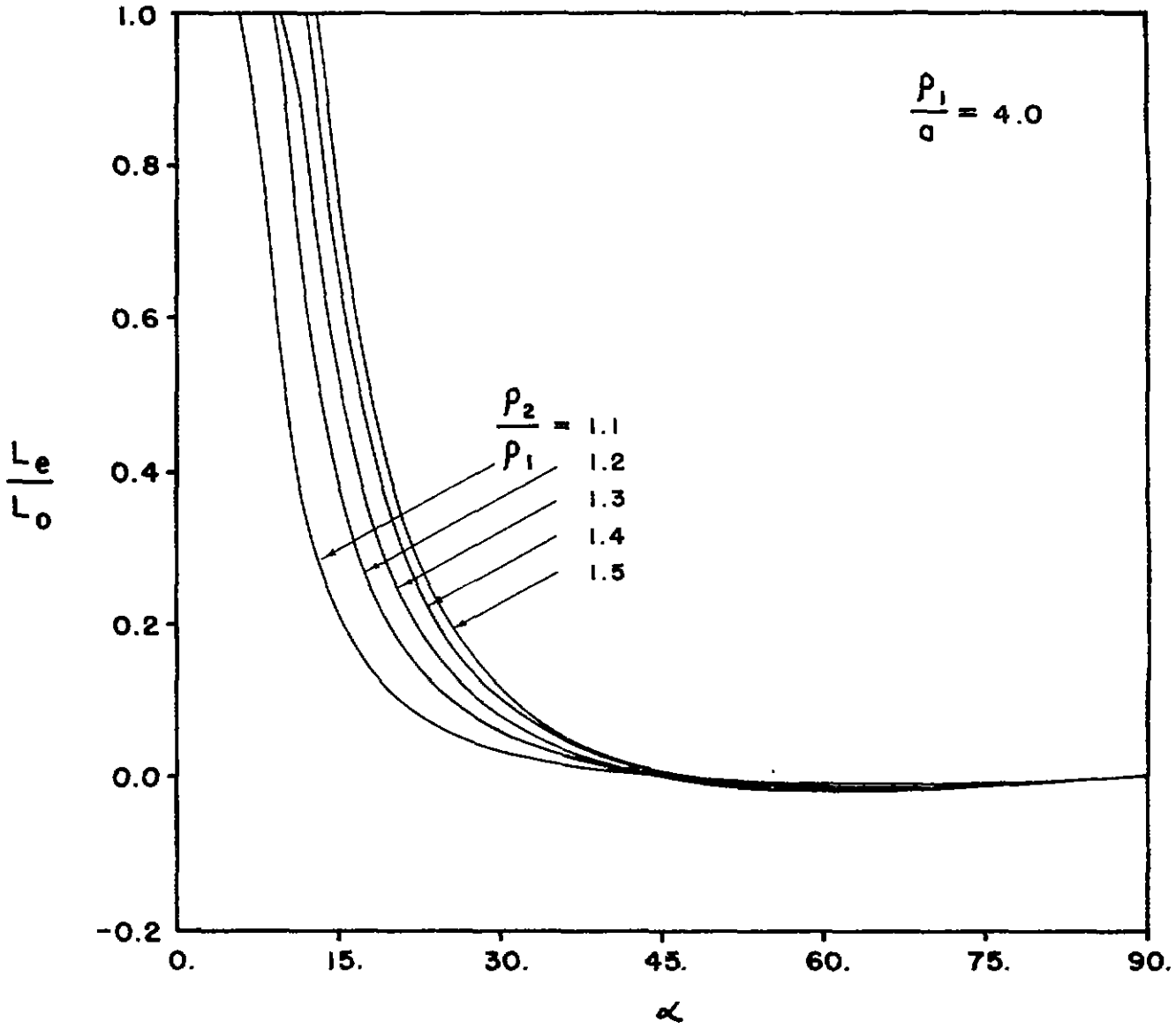

Fig. 10. Normalized external inductance per meter vs. α: $\rho_1/a = 4.0$.

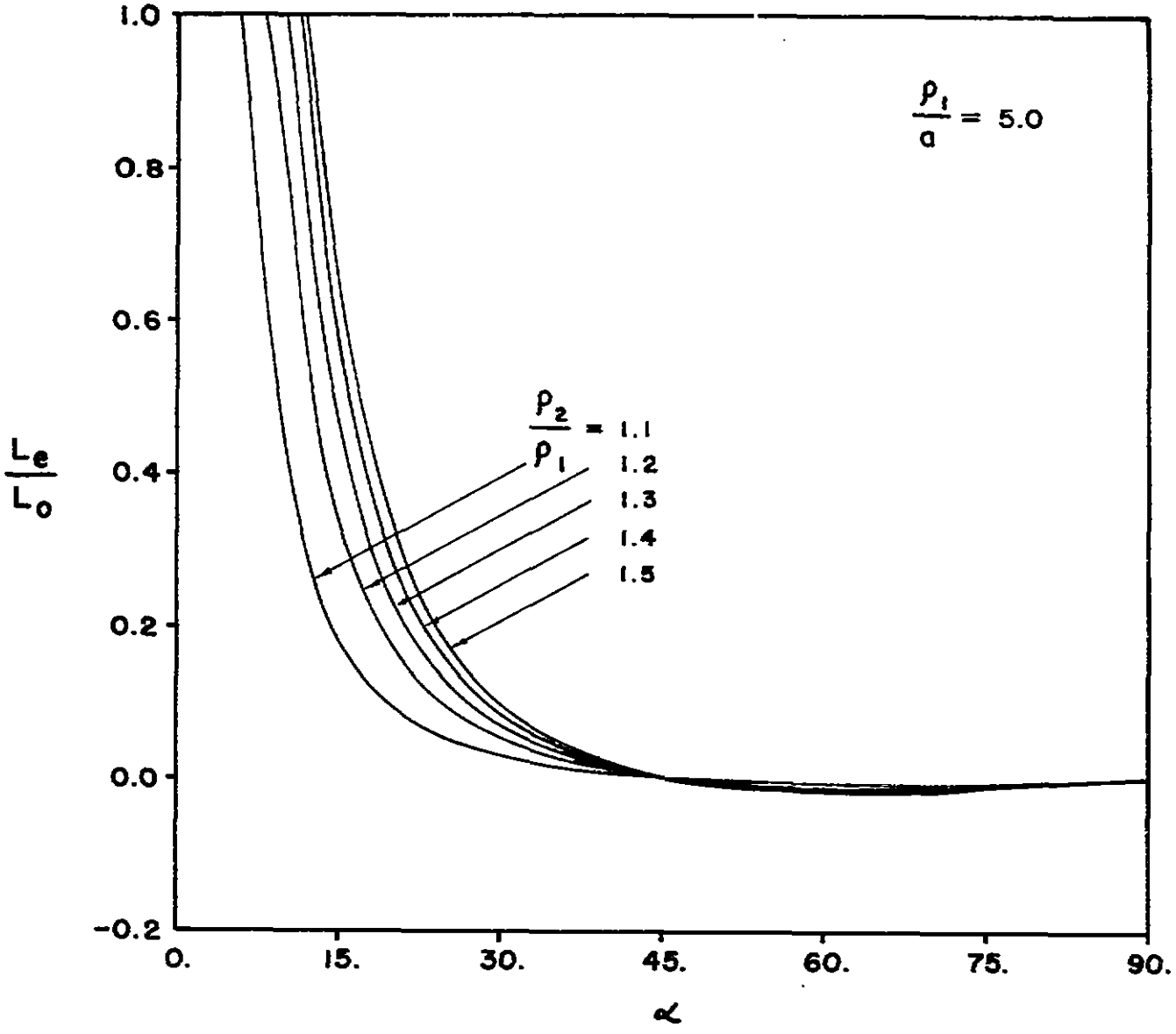

Fig. 11. Normalized external inductance per meter vs. α: $\rho_1/a = 5.0$.

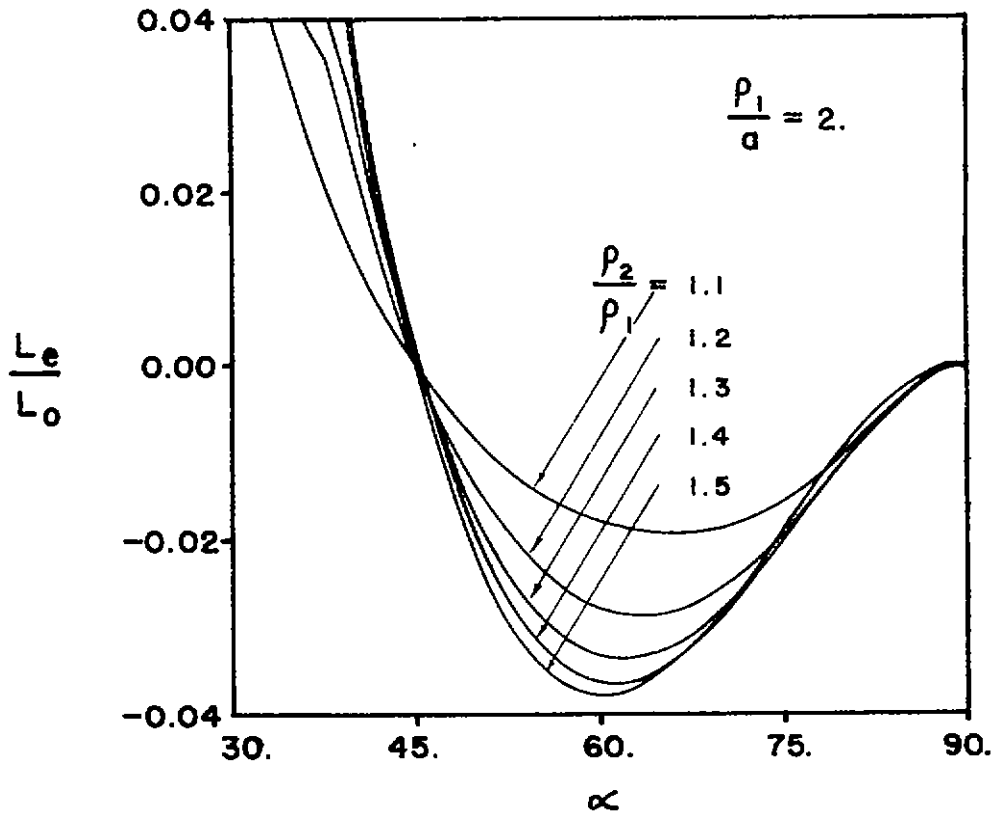

Fig. 12. Detail of Fig. (8): $\alpha \geq 30°$.

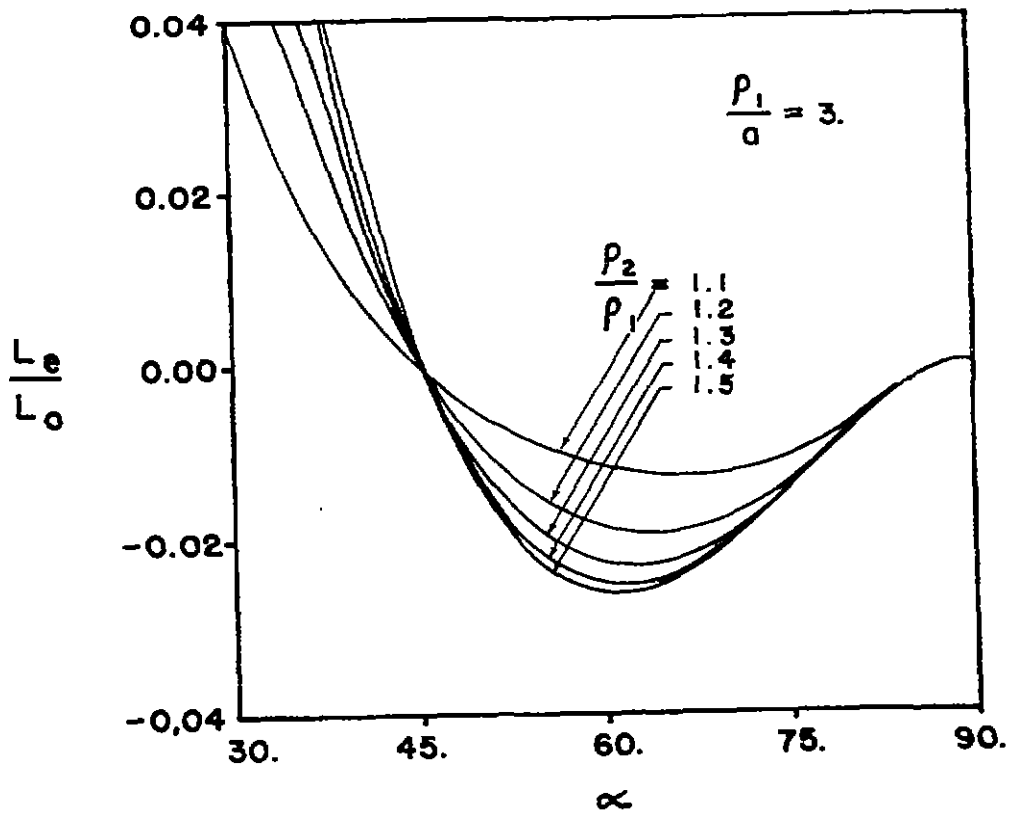

Fig. 13. Detail of Fig. (9): $\alpha \geq 30°$.

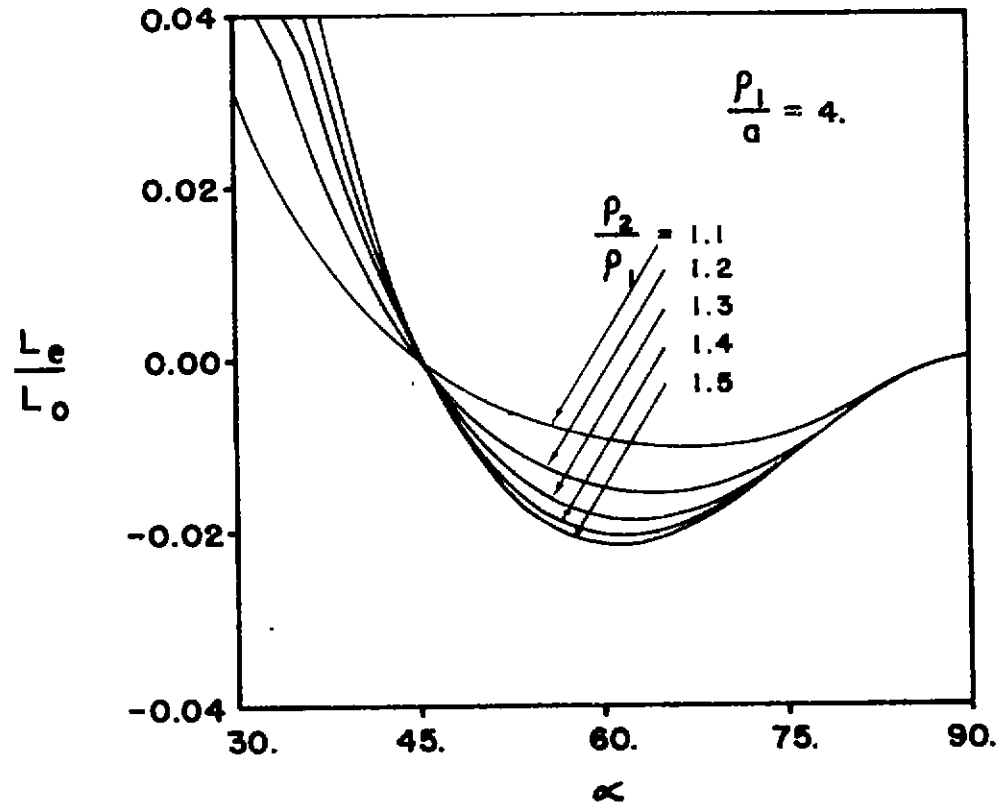

Fig. 14. Detail of Fig. (10): $\alpha \geq 30°$.

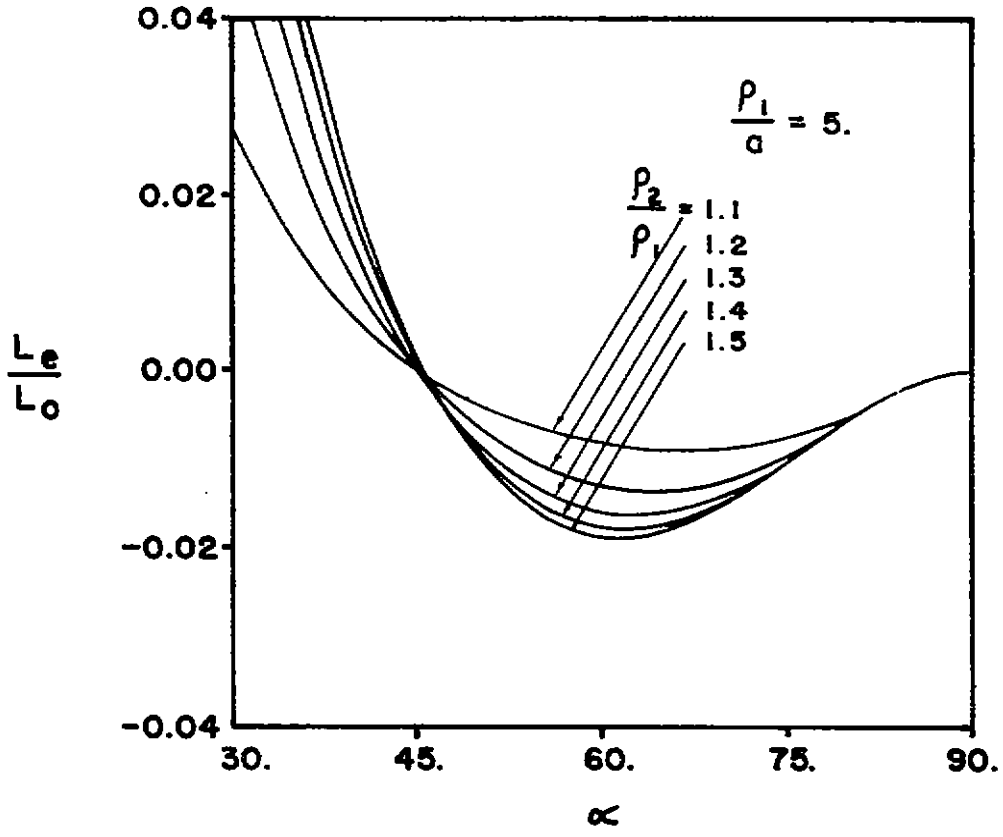

Fig. 15. Detail of Fig. (11): $\alpha \geq 30°$.

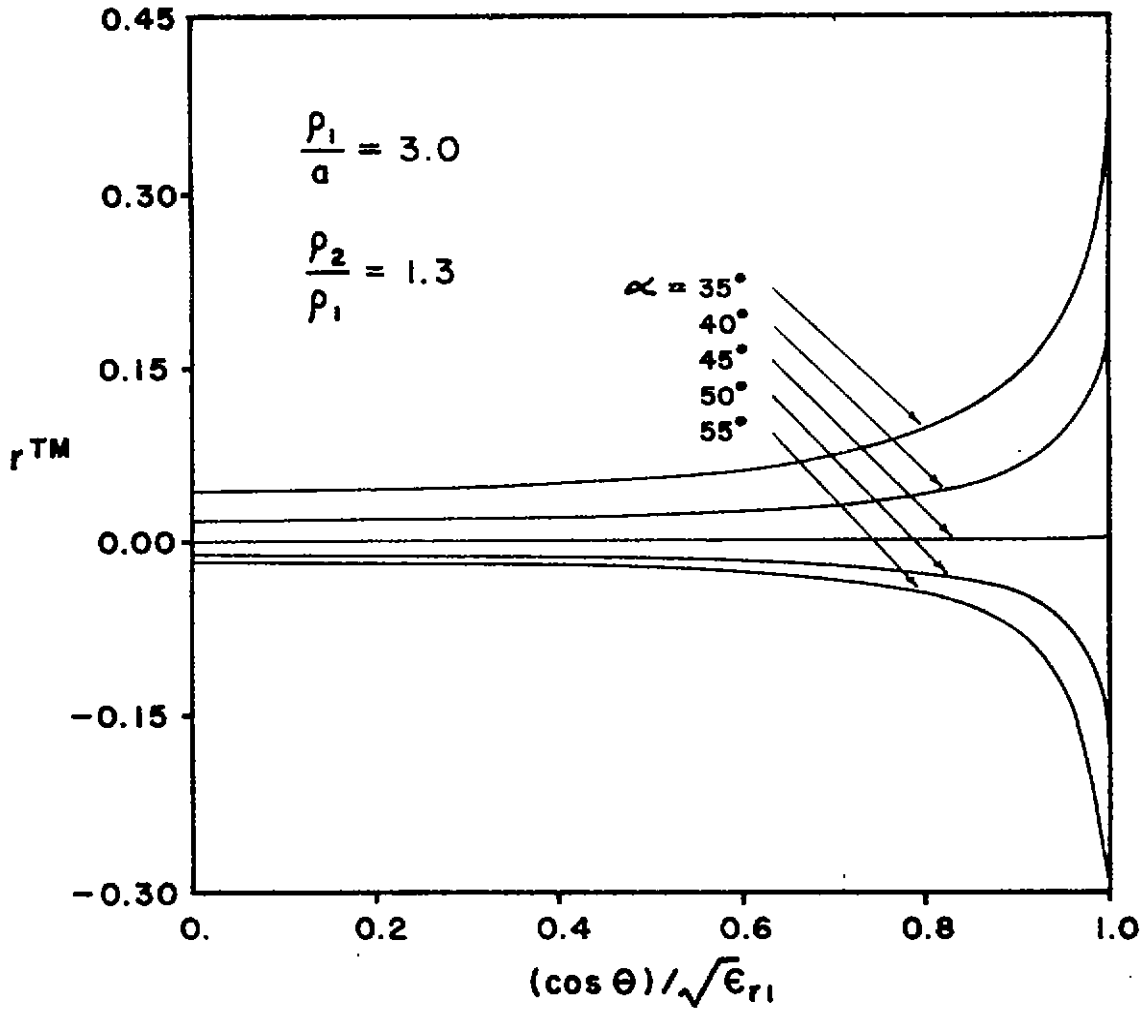

Fig. 16. Shielding factor r^{TM} vs. $(\cos\theta)/\sqrt{\epsilon_{r1}}$: $\rho_1/a = 3.0$, $\rho_2/\rho_1 = 1.3$.

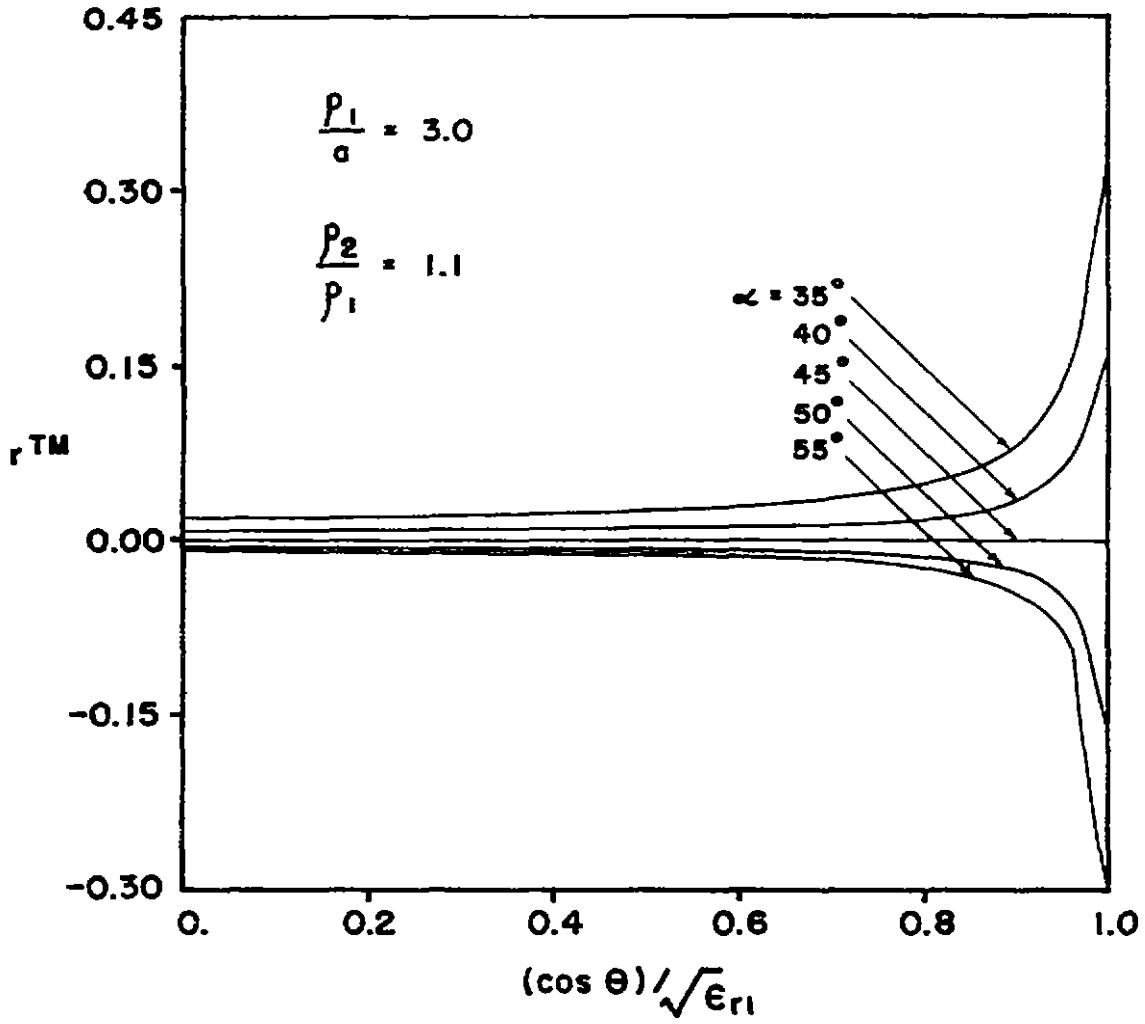

Fig. 17. Shielding factor r^{TM} vs. $(\cos\theta)/\sqrt{\epsilon_{r1}}$: $\rho_1/a = 3.0$, $\rho_2/\rho_1 = 1.1$.

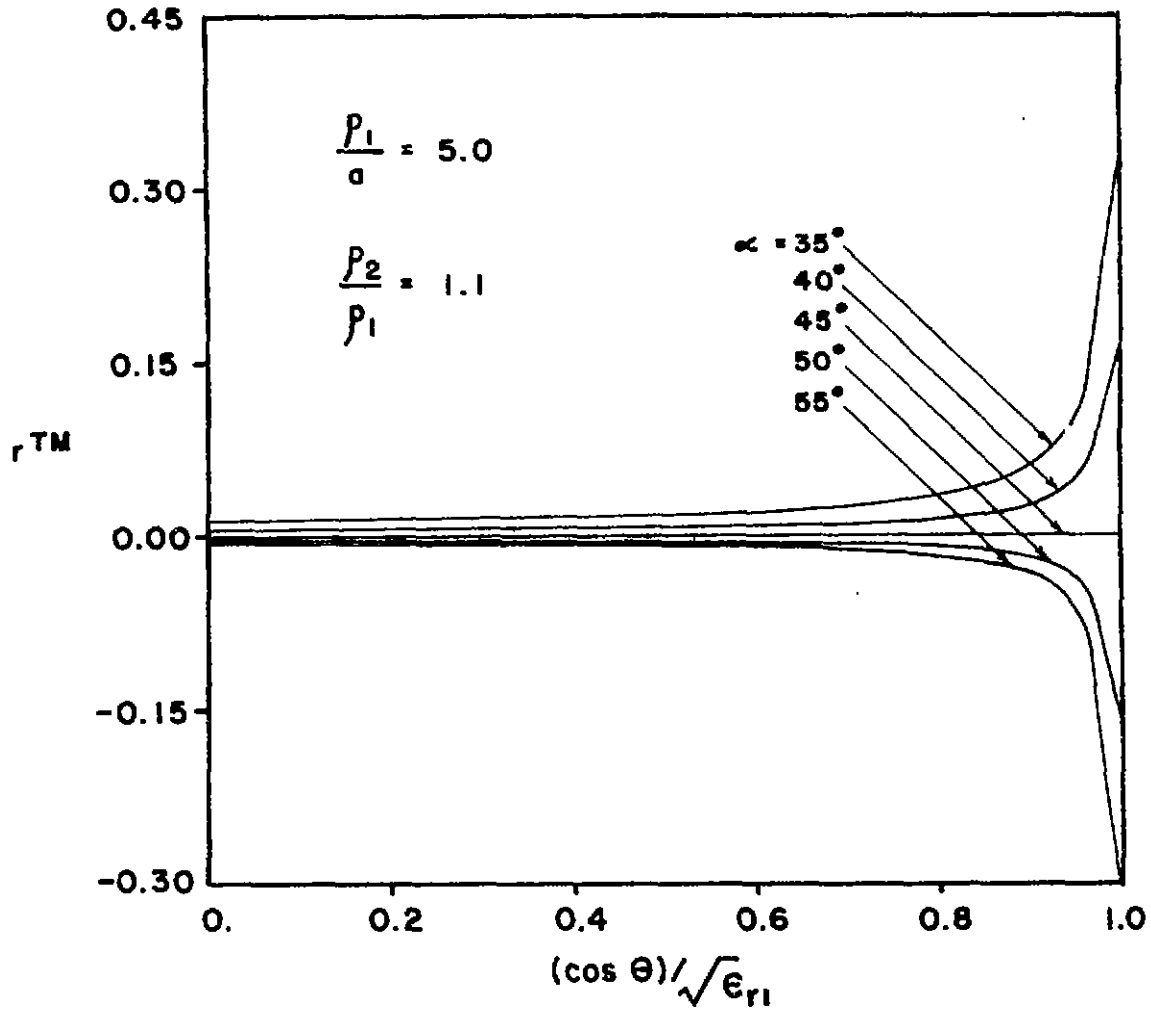

Fig. 18. Shielding factor r^{TM} vs. $(\cos\theta)/\sqrt{\epsilon_{r1}}$: $\rho_1/a = 5.0$, $\rho_2/\rho_1 = 1.1$.

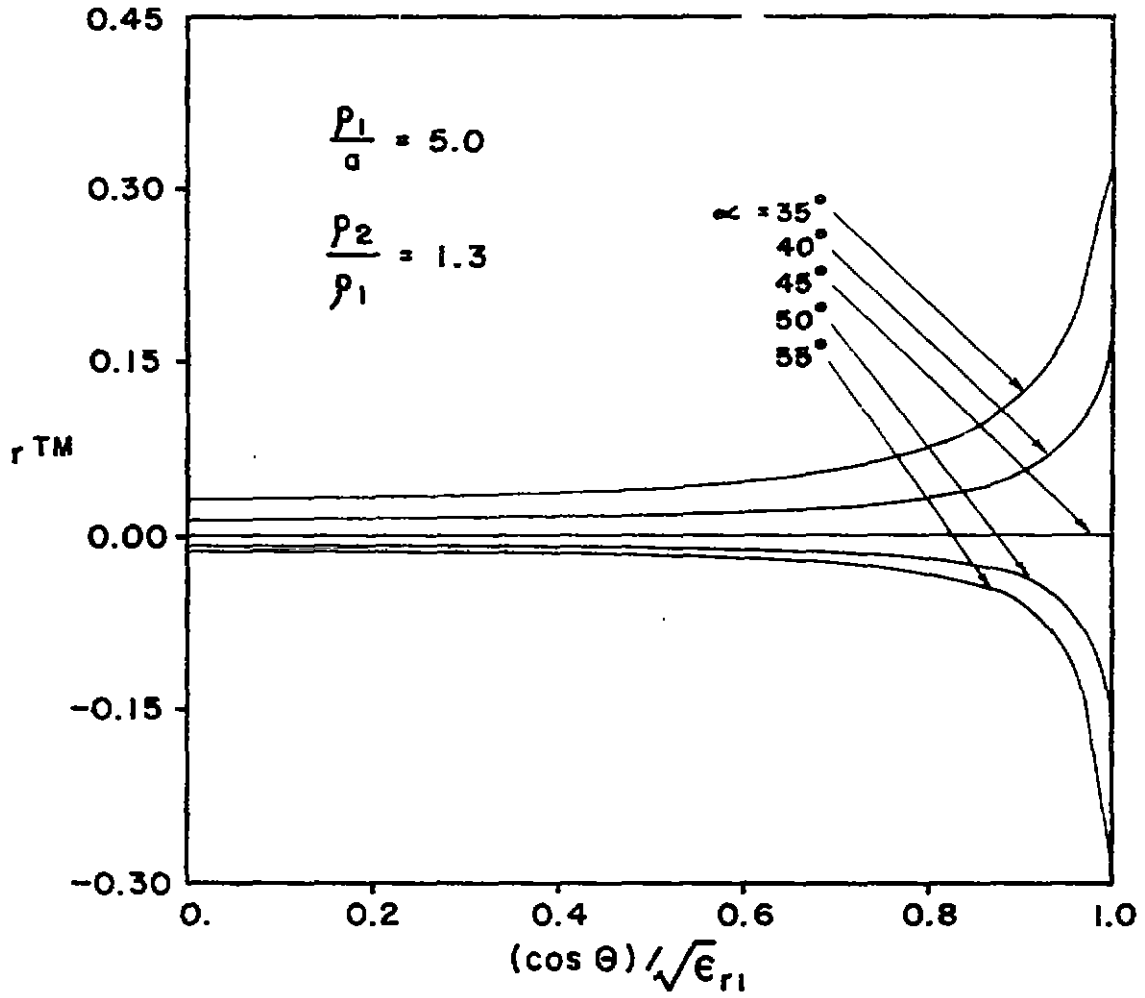

Fig. 19. Shielding factor r^{TM} vs. $(\cos\theta)/\sqrt{\varepsilon_{r1}}$: $\rho_1/a = 5.0$, $\rho_2/\rho_1 = 1.3$.

VI. Summary and Discussion

In this note we have calculated the axially symmetric part of the electromagnetic field which penetrates a certain coaxial-cable model when it is illuminated by an incident plane electromagnetic wave. The currents and voltages induced on the cable conductors were found in the low-frequency limit. It was shown that unless the incident wave is polarized with its electric vector normal to the cable axis, the induced currents (and voltages) are singular as $(\omega \ln \omega)^{-1}$. The time-domain behavior of these quantities can thus be found with the help of [1]. In the case where the incident wave is polarized normal to the cable axis, the induced currents and voltages are constant with respect to frequency in the low-frequency limit. Thus the temporal behavior of these quantities is simply that of the incident field.

The effectiveness of the two concentric unidirectionally-conducting shells as a cable shield depends principally on their conduction angles and separation. It was shown that when the conduction angles of the shells are unequal, perfect shielding is obtained when the shells have zero separation. If the separation is not zero, perfect shielding for the dominant component of the induced current is obtained if either shell (or both) conducts in the axial direction. Perfect shielding is also obtained for a cable of realistic dimensions if the conduction directions are perpendicular.

The characteristics of the model as a transmission line have also been derived. The line is a slow-wave structure for all values of the conduction angles and shell separation*, and the characteristic impedance of the line is greater than that of an ideal cable of the same dimensions. The voltage

*other than zero.

source to be incorporated into the incremental circuit model of the line has been found.

The numerical exploration of this problem has been limited by reason of time to the most important case from the practical standpoint, the counterwound cable of realistic dimensions. More extensive calculations of the case for which the conduction angles are not equal and opposite may be carried out in the future.

The question of whether or not this model accurately represents a realistic braided-shield coaxial cable is not resolved. Clearly the special case $\rho_2 = \rho_1$, $\alpha_1 = -\alpha_2$ behaves similarly to an ideal coaxial cable, the deviations from the ideal being of first order in the shell separation as long as $\alpha \neq 0°$. Yet, as was mentioned in the Introduction, the finite optical coverage of a realistic shield is not a feature of this model; and the fact that the optical coverage is not unity may turn out to be the most important source of imperfect shielding in coaxial cables.

For reference, we include in this summary the various formulas pertinent to the counterwound cable with small shell separation and α in the neighborhood of 45°. The formulas are less accurate than those given previously, but they display the effect of the shell separation and conduction angles as simply as possible under conditions of near-perfect shielding.

a) internal inductance per unit length

$$L_i \simeq \frac{\mu_o}{2\pi} \ln \frac{\rho_1}{a} \left(1 + \frac{\xi \csc^2\alpha}{4 \ln \rho_1/a}\right)$$

b) external inductance per unit length

$$L_e \simeq \frac{\mu_o \xi}{8\pi} (\cot^2\alpha - 1)$$

c) characteristic impedance

$$Z_o \simeq \frac{\eta_1}{2\pi} \ln \frac{\rho_1}{a} \left(1 + \frac{\xi \csc^2\alpha}{8 \ln \rho_1/a}\right)$$

d) propagation constant

$$k_{zt} \simeq k_1 \left(1 + \frac{\xi \csc^2\alpha}{8 \ln \rho_1/a}\right)$$

e) shielding effectiveness ($\cos^2\theta < \varepsilon_{r1}$)

$$r^{TM} \simeq \frac{\xi(\cot^2\alpha - 1)}{4 \ln \rho_1/a \left(1 - \frac{1}{\varepsilon_{r1}} \cos^2\theta\right)} .$$

Appendix

In this Appendix, we derive the voltage-change equation for the case in which the incident wave is polarized with its electric vector normal to the cable axis. We consider the source current in this case to be

$$\hat{I}_{oeq} = -2\pi\rho_2 H_o \sin\theta \tag{A1}$$

in which H_o is the amplitude of the magnetic field of the illuminating plane wave. We have

$$\frac{dV_{co}}{dz} = -j\omega L_i I_o + j\omega L_{el} I_{oeq} , \tag{A2}$$

where L_i is given in Eq. (36). Assuming that the wave is normally incident on the cable, we readily obtain

$$L_{el} = L_i \frac{I_o}{I_{oeq}} = \tan\alpha_2 L_e \tag{A3}$$

where L_e is given in Eq. (38). Thus in this special case, the voltage source in the equivalent circuit of Fig. (3) would be $j\omega \tan\alpha_2 L_e I_{oeq} \Delta z$.

References

[1] P. R. Barnes, "The Axial Current Induced on an Infinitely Long, Perfectly Conducting, Circular Cylinder in Free Space by a Transient Electromagnetic Plane Wave," Interaction Note 64, March 1971.

[2] R. E. Collin, Field Theory of Guided Waves. New York: McGraw-Hill, 1960, pp. 401-403.

[3] R. W. Latham, "An Approach to Certain Cable Shielding Calculations," Interaction Note 90, January 1972, Appendix C.